OKTOBER 1995 ECN-C--95-056

DYNAMIC INFLOW: YAWED CONDITIONS AND PARTIAL SPAN PITCH CONTROL

J.G. SCHEPERS
H. SNEL

CONTRIBUTIONS FROM:
J.G. SCHEPERS (NETHERLANDS ENERGY RESEARCH FOUNDATION)
H. SNEL (NETHERLANDS ENERGY RESEARCH FOUNDATION)
G.J.W. VAN BUSSEL (DELFT UNIVERSITY OF TECHNOLOGY)
L.J. VERMEER (DELFT UNIVERSITY OF TECHNOLOGY)
R.I. RAWLINSON SMITH (GARRAD HASSAND AND PARTNERS LTD.)
S. VOUTSINAS (NATIONAL TECHNICAL UNIVERSITY OF ATHENS)
S. HUBERSON (UNIVERSITY OF LE HAVRE)
Th. VAN HOLTEN (STORK PRODUCT ENGINEERING)
S. ØYE (TECHNICAL UNIVERSITY OF DENMARK)
H. GANANDER (TEKNIKGRUPPEN AB)
B. MONTGOMERIE (TEKNIKGRUPPEN AB, NETHERLANDS ENERGY RESEARCH FOUNDATION)
R. BAREIß (UNIVERSITY OF STUTTGART)
K. BRAUN (UNIVERSITY OF STUTTGART)

ACKNOWLEDGEMENT

The work described in this report is part of the JOULE II programme, Wind Energy, R&D of the Commission of the European Communities. The commission financed 50% of the estimate. The remainder was funded by the participating organisations and/or their national agencies.

J. Noakes from Renewable Energy Systems Ltd. is acknowledged for his help with the development of a structural model for Howden Richborough turbine.

Distribution

Commission of the European Communities:

K. Diamantaras	1 – 5
A. Russell	6
A. Zervos	7

ECN:

H.H. van den Kroonenberg	8
H.J.M. Beurskens	9
L.G.J. Janssen	10
H.J. van Grol	11
J.G. Schepers	12 – 26
Archief DE	27 – 66
Centraal archief	67

Garrad Hassan and Partners Ltd.:

R.I. Rawlinson Smith	68 – 72

SPE:

Th. van Holten	73 – 77

Technical University of Delft:

G.J.W. van Bussel	78 – 82

Technical University of Denmark:

S. Øye	83 – 87

National Technical University of Athens:

S. Voutsinas	88 – 92

Teknikgruppen AB:

H. Ganander	93 – 97

University of Stuttgart:

R. Bareiß	98 – 102
K. Braun	103 – 107

SUMMARY

This report describes the work and the results of the project 'Dynamic Inflow: Yawed Conditions and Partial Span Pitch', which is performed within the framework of the JOULE II program. The work was sponsored by the European Commision under contract and on a 50% reimbursement of the estimated total cost.

The objective of the project was to further validate the engineering method(s) of dynamic inflow which were developed in the JOULE I project 'Joint Investigation of Dynamic Inflow Effects and Implementation of an Engineering Method, JOUR 0083, see [1].

An engineering method means a model which must be easily implemented within existing wind turbine aeroelastic codes. Therefore the models should be economic in computer usage, comparable to the present generation of (steady equilibrium) inflow models. The models derived in the JOULE I project can be divided into models for axisymmetric conditions (pitching actions and wind gusts) and asymetric (yawed) conditions. Of course the combined models are able to treat pitching actions in yaw also. The validation of the models derived (and partly also the model forming) has been done on the basis of measurements on the Danish Tjæreborg turbine (60 m diameter) for pitching transients and yawed conditions and wind tunnel measurements from the University of Delft on a model turbine with diameter of 1.2 m for yawed conditions and wind gusts. Furthermore, results of the engineering methods have been compared with calculational results from advanced free wake methods.

In the present JOULE II project, a further validation of the models has taken place on basis of measurements on the Dutch WPS-30 (30 m diameter) turbine for pitching transients, the German Uniwex (16 m diameter) turbine for pitching transients and yawed conditions, and measurements in the wind tunnel for pitching transients.

A second objective was to extend the JOULE I engineering methods for partial span pitch control. These partial span pitch models have been validated with measurements on the Howden Richborough turbine and with results from the free wake methods.

In the project 8 different models have been applied, which are abbreviated in the following way:

- ECN, i.w.: ECN integral wake model, a prescribed wake model;
- ECN, d.e.: ECN differential equation model, engineering model: A model with a time derivative added to the axial momentum equation and Glauert terms [2] for the yaw modelling;
- DUT: Delft University of Technology, acceleration potential model;
- GH: Garrad and Hassan Ltd., engineering model based on Pitt and Peters, [3];
- NTUA: National Technical University of Athens, free wake Vortex Particle Method;
- TA: Teknikgruppen AB, engineering model; A model with a time derivative added to the momentum equation and Glauert terms for the yaw modelling;
- TUDk: Technical University of Denmark, engineering model. A model with

a time derivative added to the momentum equation and Glauert terms for the yaw modelling;
- Unist: University of Stuttgart, free wake panel method.

By combination of the JOULE I and JOULE II project results, a very thorough validation of the dynamic inflow models could be carried out.

The most important conclusions which can be drawn from both projects are:
- The projects have provided very useful insights in the dynamics of the induced velocities in the rotor plane and although it falls outside the scope of the project, much information about the static induced velocities was gained as well. These insights are not only relevant for wind turbine aerodynamics but also for helicopter aerodynamics.
- A clear dynamic inflow effect was observed in measured mechanical loads at full span pitching steps. It is shown that the dynamic inflow effects become more important when size and pitching speed of the turbine are increased.
- The time scale in the dynamic inflow process, which was derived from measured results, appears to be in the order of 0.5 times the ratio of the rotor diameter and the free stream wind speed.
- It is found that the models which are developed in the present project predict the response of a full span pitch regulated turbine much better. The conventional methods underpredict the load fluctuations at pitching variations.
- The dynamic inflow effects for turbines with partial span pitch control appeared to be limited. It is shown that the pitching of the tip does not influence the induced velocities on the inner, fixed, part of the blade, i.e. radial independency is valid, which means that steady equilibrium methods would give a sufficiently good approximation for most purposes.
- The dynamic inflow effects for coherent wind gusts appeared to be very limited. This was derived from theoretical considerations, and confirmed by wind tunnel measurements.
- It is found that the skewed wake effects the phase and amplitude of the azimuthal binned averaged flatwise moment. This is in particular true at situations when the loading (the axial induction factor) and the tip speed ratio are large
- It is shown that the conventional models do not correctly predict the flatwise and yawing moment on a wind turbine under yawed conditions. The yawing moment has negligible values when calculated with the conventional methods. The newly developed engineering models, calculate at least the sign and the order of magnitude correctly (with a limited computational time), which is very important for the design of free yawing wind turbines.
- Direct evidence of dynamic inflow effects was obtained from wake flow field measurements, performed in the DUT wind tunnel at pitching steps and yawed conditions. The free wake methods were able to reproduce the wake flow field measurements very accurately. The engineering methods are not suited to perform that kind of calculations.
- A surprising result was that the skewed wake does not only influence the axial induced velocities (which was expected from helicopter aerodynamics), but also the lateral induced velocities. This could be reproduced with the free wake methods. In the cases which have been considered, the practical importance of this effect is limited.
- It is recommended to replace the conventional steady equilibrium wake methods by one of the engineering methods from the present project.

Apart from ad-hoc presentations and presentations at JOULE contractor's meet-

ings, intermediate results were presented at the:

- EWEC conference in October 1991 in Amsterdam [4];
- ECWEC conference in March 1993 in Travemunde [5];
- European Rotorcraft Forum in October 1994 in Amsterdam [6];
- EWEC conference in October 1994 in Thessaloniki [7];
- Journal of Wind Engineering and Industrial Aerodynamics [8]

CONTENTS

1. INTRODUCTION

This report describes the results from the JOULE II project 'Dynamic Inflow: Yawed Conditions and Partial Span Pitch Control (JOU2-CT92-0186). This JOULE II project is the sequel of the JOULE I project 'Joint Investigation of Dynamic Inflow Effects and Implementation of an Engineering Method for Response Calculations', [1] (JOUR 0083-C)

In the JOULE I project, models were derived to describe dynamic inflow, i.e. the instationarities and non-uniformities of the inflow velocities in the rotorplane, induced by the trailing wake vorticity, such as result from blade pitch actions, wind gusts and yawed flow conditions. Trailing wake vorticity is the result of varying circulation strength along the blade axis; it also exists in the stationary case. It is especially strong where the radial changes are important, i.e. near the blade tip and the blade root. The characteristic time scale for this phenomenon is D/V_∞. Phenomena having a time scale large compared to this may be regarded as quasi steady.

In the JOULE I project, dynamic inflow effects were investigated for:
- coherent wind gusts ;
- full span pitching actions ;
- yawed operation.

The models derived in the JOULE I project can be divided into models for axisymmetric conditions (pitching actions and wind gusts) and asymmetric (yawed) conditions. Of course the combined models are able to treat pitching actions in yaw also. The validation of the models derived (and partly also the model forming) has been done on the basis of measurements on the Danish Tjaereborg turbine (60 m diameter) and wind tunnel measurements from the University of Delft on a model of 1.2 m diameter, certainly two extremes of the size range.

The models were implemented in the aeroelastic codes that are used by designers for the determination of system dynamics and of the load spectrum of turbines. Apart from these models (referred to as 'engineering models'), a group of free wake programs participated in the project. These models have been used to obtain flow field information to check the assumptions used in the engineering methods.

The investigation of yawed conditions was added as an extention to the JOULE I project and therefore the JOULE I and JOULE II projects ran in parallel for some time. The participants of both projects were the same.

In the present project, the JOULE I models have been further validated, by considering turbines with different sizes than those from the JOULE I project. The following situations have been adressed:
- Full span pitch transients on the WPS-30 turbine with rotor diameter of 30 m.
- Full span pitch transients and yawed flow on the Uniwex turbine with rotor diameter of 16 m.
- Measurements on the DUT wind tunnel model, exposed to full span pitching steps. These measurements appeared to be very useful, not only because of the stable and controlled conditions, but also because the wake flow field was measured during the pitching transients. In the JOULE I pitching step measurements, mechanical loads are measured only. Since the wake determines the dynamic inflow effects, the present measurements give more direct validation

material for the dynamic inflow models.

Consequently, the combination of the JOULE I and JOULE II project results yields a very complete validation of dynamic inflow models, since the turbine diameters range from 1.2 m (wind tunnel), 16 m (Uniwex), 30 m (WPS-30) and 60 m (Tjaereborg).

Another limitation which was made in the JOULE I project, was the restriction to full span pitch situations. In the present project, the models have been extended to the situation of partial span pitch. Thereto a (limited) comparison is made with partial span pitch measurements on the Howden Richborough turbine (D = 55 m). Verification of the engineering models for partial span pitch has also taken place by comparing with results from advanced free wake methods from NTUA and Unist.

Due to the very strong relationship between the JOULE I and JOULE II projects, this report includes a brief summary of the most important results of the JOULE I project in chapter 5. Those parts of the JOULE I report, which are considered essential for a good understanding of the present report, have been copied completely into this report. These are the short descriptions of the full span pitch and yaw models, which are described in section 7 and 14.

The full span pitching step results are described in section 8 (WPS-30 turbine), section 9 (Uniwex turbine) and section 10 (DUT wind tunnel model). The latter measurements were originally scheduled for the JOULE I project, but were not completed in time. Therefore they are described in the present report.

The reporting of the full span pitch cases is followed by the partial span pitch cases, in section 12 (model description) and 13 (results).

Thereafter the yawed measurement on the Uniwex turbine are described in section 15.

The notations and conventions which are used in the JOULE II project are, apart from some small modifications, similar to those which are applied in the JOULE I project. They are given in Appendix A. Unless otherwise stated, these notations and conventions are used.

2. OBJECTIVE OF THE PROJECT

The objective of the project is:

- To further validate the dynamic inflow models, described in [1] on machines of intermediate sizes (The 30 m diameter WPS-30 and the 16 m diameter Uniwex).
- To further develop the pitching transient type of dynamic inflow models, described in [1] to the partial span pitch situation and validation on basis of comparison with measurements on the Howden Richborough turbine and calculational results from advanced free wake models.

The result should be a validated 'second generation' aerodynamic model which accounts for wake induced instationarities and non-uniformities, and that can replace the standard blade element moment methods with steady equilibrium wake assumptions that have been the core of aeroelastic programs until now.

3. PARTICIPANTS

The following parties participated in the project:

- Netherlands Energy Research Foundation (ECN), NL (coordinator) together with Stork Products Engineering (SPE) NL;
  KEMA acted as a subcontractor of ECN.
- University of Stuttgart (Unist.), FRG;
  - Institut fur Aerodynamik und Gasdynamik;
  - Institut fur Computer Anwendungen.
- National Technical University of Athens (NTUA), Gr, together with Laharatoire de Mecanique des Fluides, University of Le Havre (F);
- Garrad Hassan and Partners Ltd (GH), UK;
- Delft University of Technology (DUT), NL;
- Technical University of Denmark (TUDk), Fluid Mechanics Department Lyngby
- Teknikgruppen, AB (S)

4. WORK PROCEDURE

Four different types of work can be distinguished:

1. Further validation of engineering model(s) for dynamic inflow at full span pitch and yawed conditions.
2. Development, implementation and validation of engineering model(s) for dynamic inflow at partial span pitch conditions.
3. Use of the free vortex models in order to obtain phenomenological insight in flow features and to (partially) validate the engineering models.
4. Supply of dedicated full scale and wind tunnel measurements, for the validation of the models.

The methodology followed in the project is for a large part similar to the one which is followed in the JOULE I project. It can be characterized as follows:

- Specific measurements were requested from the WPS-30 and Uniwex turbine (full span pitching transients and yawed flow measurements). These measurements have been reproduced with the engineering methods, developed in the JOULE I project and the free wake methods.
- On a voluntary basis, windtunnel measurements (blade loads and wake flow field) for full span pitching transients have been reproduced with the engineering methods, developed in the JOULE I project and the free wake methods. These measurements delivered insight in the wake development during a pitching transient.
- The existing full span pitch dynamic inflow engineering models, have been evaluated to make them suited for partial span pitch control. These models are described and explained in chapter 12.
- For partial span pitch conditions, testcases were defined in which results of the engineering models were compared mutually and with results of free vortex wake calculations. For these cases, purely aerodynamic quantities were calculated, i.e induced velocities and aerodynamic loads. Insight gained in this way was very instrumental in the model development.
- Unfortunately no new measurements could be obtained from the Howden Richborough turbine, and so existing measurements were used and simulated with the calculational models.

The experimental configurations (i.e. the Uniwex, the WPS-30, the Howden Richborough turbine and the wind tunnel model) are detailed in chapter 6. The WPS-30 pitching transient measurements are described in chapter 8.1. This is followed by a description and evaluation of the different calculational cases carried out on the WPS-30 geometry in chapter 8.2 and 8.3. The WPS-30 cases are denoted by case WII; An additional case, (case WI.2) is described in this report also, at a wind speed higher than the one of the measurement cases. Case WI.2 is analysed by means of calculational results only. The description and evaluation of the pitching transients carried out on the Uniwex geometry are given in chapter 9.2 and 9.3. The Uniwex pitching step cases are denoted by case UI; Two cases at two different ambient wind speeds and pitch angles have been simulated. In addition a stop case of the Uniwex turbine has been simulated. This case is denoted by case UIII.

The wind tunnel pitching transient measurements are given in section 10.1. This case is denoted by case tun-pitch. There are three different cases at three different

wind speeds. The description and analysis of these results is given in 10.2 and 10.3.

The partial span pitch cases are described in 13.2 and 13.3. There are two cases, denoted by case HI and case HII. Case HI gives an artificial step on the tip angle, for two different wind speeds on the Howden Richborough geometry. Case HII gives the simulation of a start-up which is measured on the Howden Richborough turbine. The measurement campaign is described in section 13.1.

The Uniwex measurements under yawed conditions are described in section 15.1. The description and analysis of these cases are given in section 15.2 and 15.3. The calculational case is denoted by case UII: Two measurement series were reproduced at yaw angles of approximately $\pm$ 45 degrees. Azimuthal binned averaged values have been compared.

The group of participants met with a frequency of approximately 3 times per year. These meetings were combined with the meetings from the JOULE 1 project. During these plenary meetings, model features were presented and discussed. Measurement campaigns were defined, discussed and results thereof were presented. Calculational results were compared with measurements and interpreted. The main items of each meeting are recorded in the minutes, by the coordinator.

Within the course of the project, it appeared to be very difficult but also very useful to get consensus about sign conventions and definitions. Agreement was reached on the conventions given in Appendix A. Unless otherwise stated, the conventions from this Appendix are used.

5. SUMMARY OF JOULE I PROJECT RESULTS

5.1 Discussion of available measurements and calculational results

5.1.1 Pitching steps

In the JOULE I project, pitching transients were supplied from the Tjæreborg 2 MW turbine. Some global characteristics of this turbine are listed below.

Diameter	61 m
Hub height	60 m
No. of blades	3
Tilt angle	3 °
Cone angle	0 °
V_{rated}	15 m/s
P_{rated}	2 MW
Ω	22.3 rpm

A total of 6 different pitching transients have been measured at different ambient wind speeds, (and consequently different loading situation of the turbine), different variations in pitch angle and different pitching speeds. In these transients, after an initial period, the blade pitch angle is first increased at a fast rate over 2 or 3°, next maintained constant for about 30 seconds and then decreased to its initial value at a fast rate. The measurement period extends over a total of 60 seconds. Measured values for blade and shaft loads have been averaged over a number of realisations, and over the three blades in order to filter out stochastic wind influences and deterministic effects as (average) wind shear and tower shadow. The averaging process is described in [9] and is repeated below:

First the time trace for the pitch angle is searched for the times where it crosses upwards through the level of the initial pitch angle. The complete time series is then divided into a number (say N) segments of 30 seconds duration, each starting 5 sec. before the level crossing. A new time series is constructed as the average of these N time series in the sense that the value of each sensor signal at a given time is the average of the N individual values from the N time series at the same time relative to the pitch angle level crossing. A new sensor signal is calculated as the mean value of the 3 averaged flatwise moments (of all three blades) to further reduce the influence of turbulence, wind shear and tower shadow. This procedure is repeated for the decreasing pitch steps determined as crossing down through the second value of the pitch angle. The resulting averaged time series is then appended to the first, starting at t=30 seconds.

Then these filtered measurements, have been simulated with the calculational methods, in which axisymmetric, stationary wind conditions have been assumed (no wind shear, no turbulence).

Table 5.1 shows the conditions pertinent to the measurements in order of decreasing λ, together with the case identification which was used in the JOULE I project. The wind speed is the average value for the case, θ_1 is the initial and final blade pitch angle, θ_2 the intermediate one after the pitch step. The value of Δt gives the

time in seconds used for the both pitching changes. Also indicated in this table are calculated values of the equilibrium induction factors a_1 and a_2 at 70 % span, to give an indication of the loading situation.

Table 5.1 *Conditions of the Tjæreborg pitching step measurements*

case	λ [--]	U [m/s]	θ_1 [°]	θ_2 [°]	Δt [s]	a_1 [--]	a_2 [--]	Ω [rpm]
II.1	9.5	7.4	1.0	3.0	2.0	0.35	0.27	22
II.4	8.1	8.7	0.1	3.7	0.5	0.34	0.23	22
II.3	7.8	9.0	0.2	3.4	long/0.6	0.33	0.22	22
II.5	7.8	9.1	-0.4	2.5	2.07	0.4	0.26	22
II.6	6.6	10.5	0.2	3.9	0.74	0.31	0.21	22
II.2	5.6	12.5	1.2	3.2	1.3	0.22	0.19	22

The indication 'long' for the Δt of case II.3 refers to the fact that the first pitch change was done with an exponential rate, with a rather steep initial value, but slowing down in the end, so that the entire pitch change takes about 3 seconds, in contrast to the second step (back to initial) which is done in 0.6 seconds.

For the lowest λ case (case II.2, λ=5.6) the inner part of the blade is in stall. This is reflected in the low values of the induction factor, which does not undergo a major change. For case II.1 (highest λ, 9.5) the rotor is partly in the turbulent wake state. This is also true for case II.5 ($\lambda = 7.8$), due to the negative pitch angle. The other cases have a λ near to the design value. All these cases are high loading cases with induction factor values of 0.33 and above, changing by approximately 30 %. Case II.4 has the highest pitching rate. The values of the pitching rate covered, vary between $1°/s$ (case II.1) and $7.2°/s$ (case II.4).
Figure 5.1 shows as an example, the response of the flatwise moment for case II.4, measured as well as calculated. The calculated result from a new engineering method, developed in the JOULE I project, and from a conventional equilibrium wake model are presented. The result for case II.2 (with lowest loading) is presented in figure 5.2. Figure 5.1 clearly shows that the new engineering method predict the response of the flatwise moment much better for a step on the pitch angle: The large overshoot after the step on the pitch angle is not predicted at all with the conventional method, but the new model predicts the magnitude and the decay of the overshoot very well. Section 7.1 gives the explanation for the difference between the calculated result from the new engineering method and the conventional equilibrium model: The dynamic inflow model takes into account the time lag in induced velocity, after the loading situation on the blade is changed due to the pitching. The conventional method, however, assumes that the new equilibrium value of the induced value is reached immediately after the pitching step. Consequently, just after the pitching step, the induction from the dynamic inflow model is different from the value calculated with a conventional method. After a certain period the dynamic inflow model yields the same equilibrium value for the induced velocity and consequently the same load level as the conventional method.

Figure 5.2 shows hardly any dynamic inflow effect on the Tjæreborg turbine for case II.2. This is explained by the very low values of the induced velocities

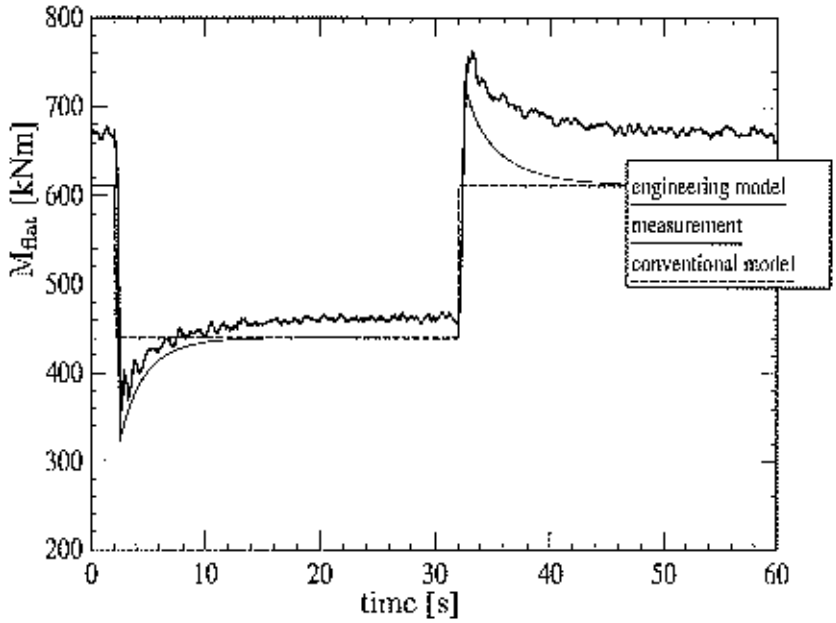

Figure 5.1 *Pitching step on Tjaereborg turbine, case II.4*

compared to the free stream wind speed. The differences in induced velocity between the conventional and the dynamic inflow model are dominated by the much larger value of the free stream wind speed and therefore the axial induction factor hardly changes due to the pitching step.

It has been attempted to determine the time constant in the dynamic inflow process for all of the cases which are listed in table 5.1. Thereto the load time series were represented by an exponential decay, according to:

$$F(t) = F_1 + \Delta F * (1 - \exp^{-(t-t_1)/f(t)}) \tag{5.1}$$

(see figure 5.3).

Then the time scale can be derived from:

$$f(t) = -\frac{t - t_1}{\ln((F_2 - F)/\Delta F)} \tag{5.2}$$

The definition of t_1, F_1 and F_2 (and consequently t_2) has been a point of concern, because the resulting time scale was very sensitive to these definitions: Figure 5.4 shows that for t_1 the time when the load is minimum or maximum is taken.

In most cases, for t_2 the time at the end of the pitching step was applied. However in some cases, rather large variations in the measured time serie occurred at the end of the pitching step. This resulted in unrealistic values for F_2. Then the value of t_2 had to be determined 'by eye'.

The fluctuations in the measured time series resulted in large fluctuations of the time scales. Therefore the time scales were approximated with a least square fit.

In figure 5.5, the time scale of the measured flatwise moment of case II.1 is derived with equation 5.2 and the resulting values are approximated with a least square

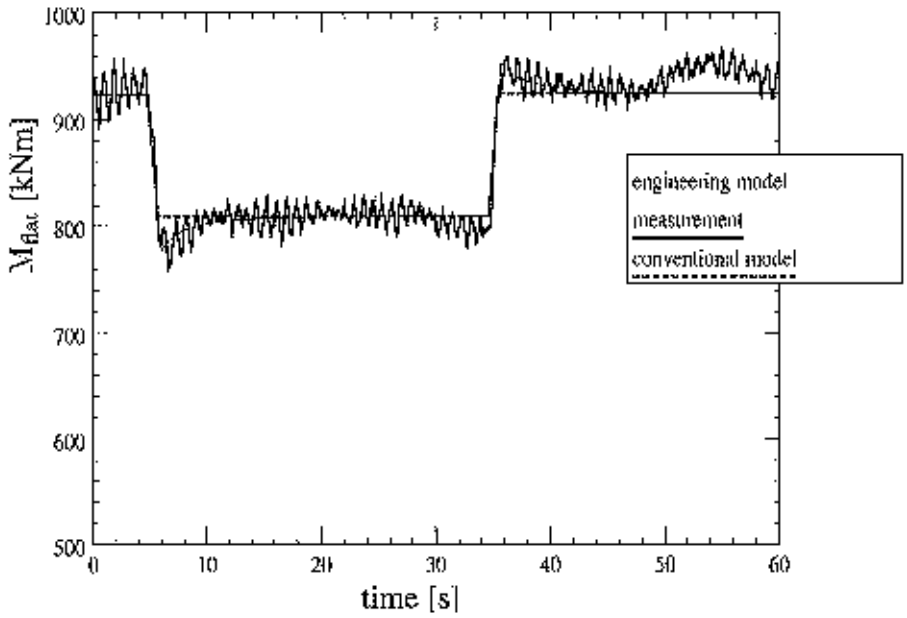

Figure 5.2 *Pitching step on Tjaereborg turbine,case H.2*

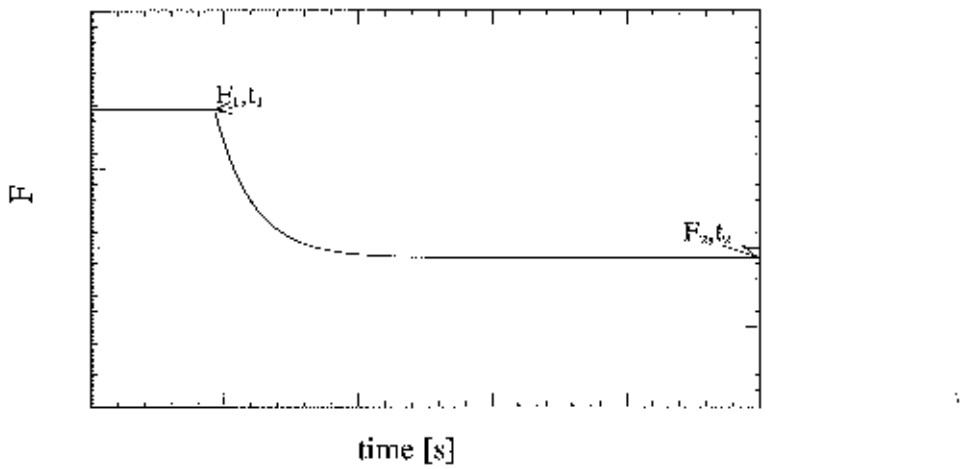

Figure 5.3 *Exponential behaviour for calculation of time scale*

fit. It can be seen that the time scale is a function of time. Therefore, reference has always been made to the time scale in the dynamic inflow process, instead of the time constant. In figure 5.6, the least square fit for the time scale is substituted in equation 5.1 and compared with the original measurement time series.

In order to compare the time scales for the different measurements in a consistent way, they were all summarized by using the value at a time of 0.5 D/V_∞ after the pitch angle had reached its new value, which is approximately $t_1 + 0.5D/V_\infty$ in figure 5.4. The resulting time scales then all lie within the range of 0.3 to 0.5 D/V_∞.

As stated above, the exact equilibrium values in the measurements have been

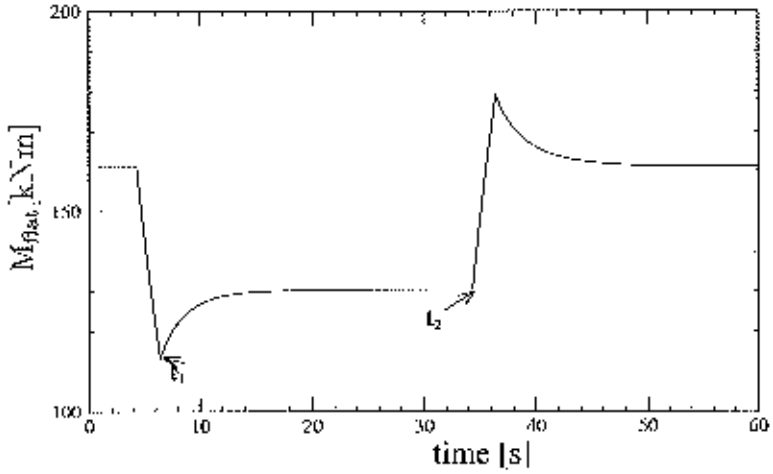

Figure 5.4 *Determination of t_1 and t_2 of flatwise moment for calculation of timescale*

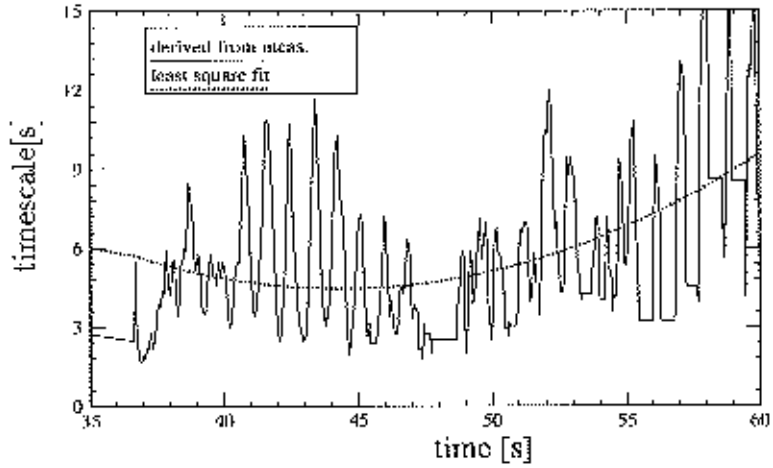

Figure 5.5 *Tjæreborg; Least square fit for time scale derived from measured flatwise moment; V_∞ = 7.4 m/s; θ = 1.0° to 3.0°; (CASE II.1)*

manipulated in some cases. This of course gives an uncertainty in the value of the measured time scale. The effect of a small change in the second equilibrium value on the time scale is shown in figure 5.7. In this figure the time scales for case II.1 are calculated with the second equilibrium value taken as the measured value at t = 60 seconds and at t = 59.44 seconds. If the resulting time scales are substituted in equation 5.1, the effect on the time serie appears to be rather limited, see figure 5.8.

However, the different equilibrium values result in a maximum difference in time scale of $0.2D/V_\infty$ while the gradient df/dt changes sign.

The measurements also showed the largest dynamic inflow for the highest pitching speed. This can be expected, since for a low pitching speed the differences between the flow conditions for any particular time interval is small and therefore dynamic inflow effects are also small.

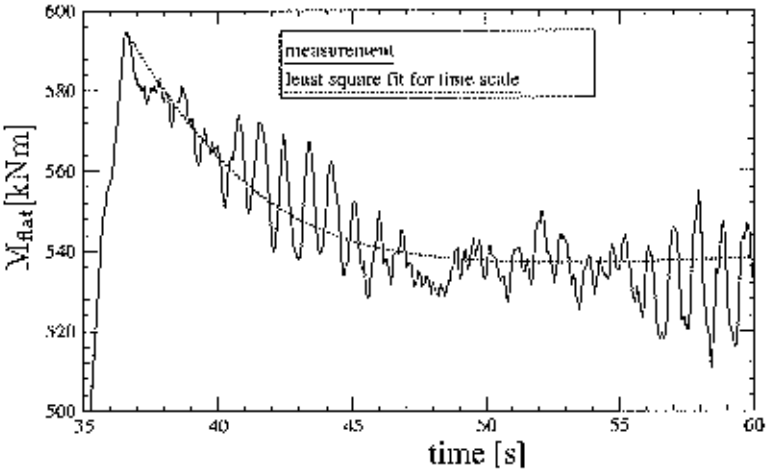

Figure 5.6 *Tjæreborg; Measured flatwise moment and approximated flatwise moment with least square fit of time scale; V_∞ = 7.4 m/s; θ = 1.0° to 3.0°; (CASE II.1)*

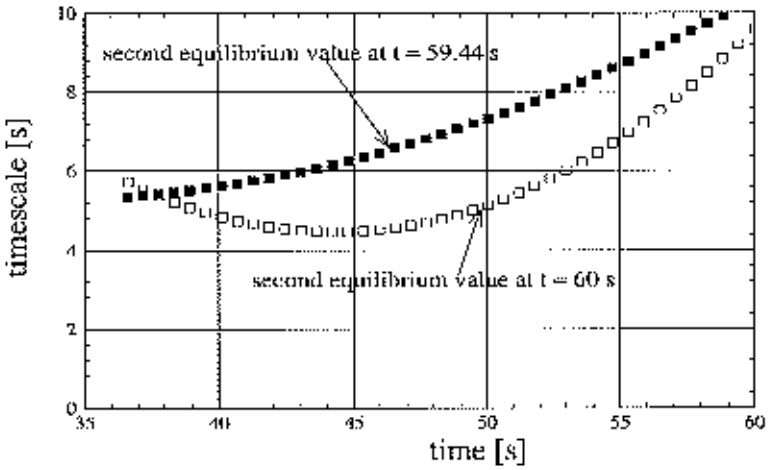

Figure 5.7 *Tjæreborg; Effect of different equilibrium values on time scale of flatwise moment; V_∞ = 7.4 m/s; θ = 1.0° to 3.0°; (CASE II.1)*

5.1.2 Wind gusts

As already explained in the introduction of this report, section 1, it was expected that dynamic inflow effects would not only be important for pitching variations, but also for wind gusts. The reason is that a change in wind speed was thought to yield a similar change in loading situation as a change on the pitch angle.

The dynamic inflow effects for wind gusts have been investigated by considering an artificial step on the wind speed for the Tjæreborg turbine. In this case, the initial wind speed was 13 m/s. The wind speed remained constant at this value for 6 seconds after which it stepped to 10 m/s. 34 Seconds later the wind speed stepped back to 13 m/s. It is obvious that this case could only be studied by mutual comparison of calculational results, since this artificial event will not occur in the free stream.

However the wind tunnel environment at the University of Delft, see section 6

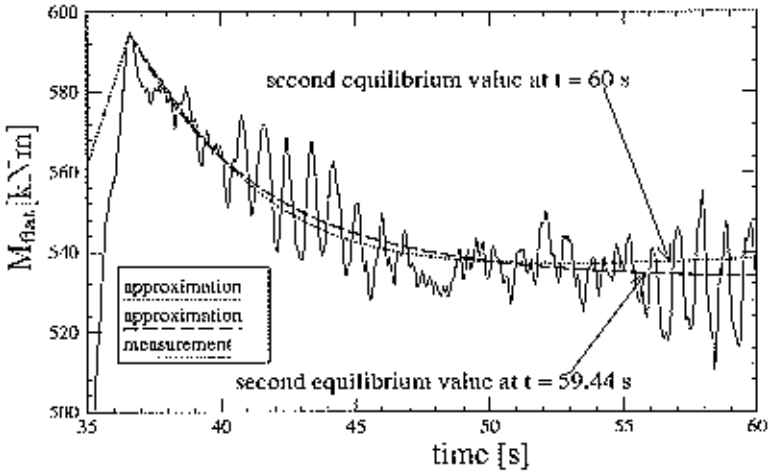

Figure 5.8 *Effect of different equilibrium values on flatwise moment; V_∞ = 7.4 m/s; θ = 1.0° to 3.0°; (CASE II.1)*

offered a unique environment to generate a step on the wind speed and to measure the response (flatwise moment) of a 1.2 m diameter turbine on it. The coherent wind gusts were realised by means of two gauzes, which could manually be opened or closed by which porosity, and therefore the wind speed, was modified. The wind speed changed from 5.7 to 4.9 m/s and vice versa within a period of 0.4 s. Figure 5.9 shows the result for the flatwise moment for the step on the wind speed going down. It can be observed from figure 5.9 that the dynamic inflow effect for

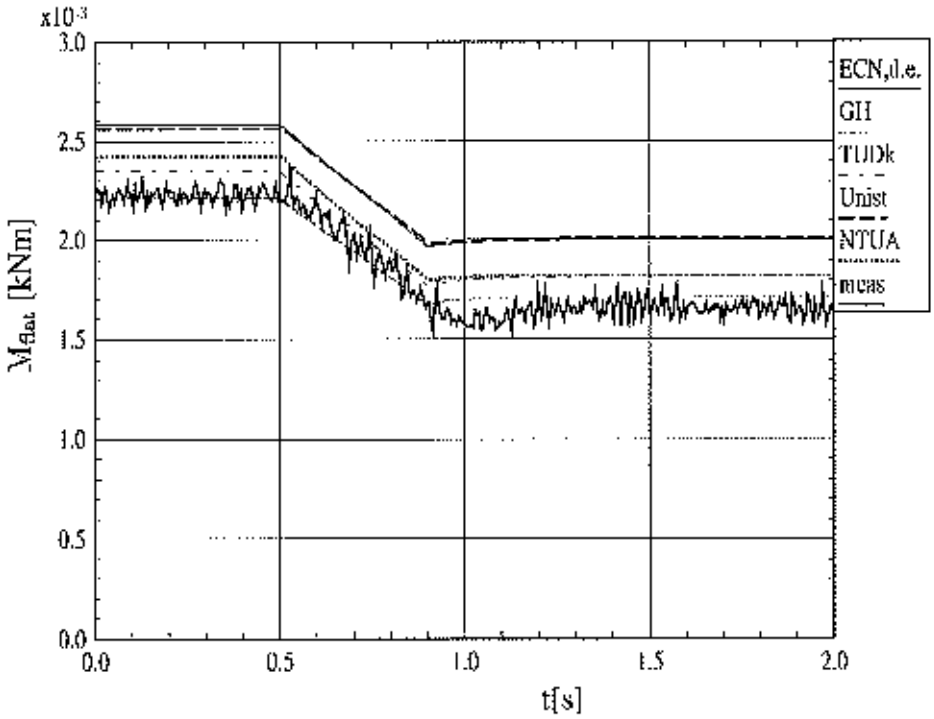

Figure 5.9 *Windtunnel, Flatwise moment; V = 5.7 to 4.9 m/s (Case tungust-down)*

a step on the wind speed in the wind tunnel is very small. Both calculations and measurements show no, or hardly any notable overshoot in the loads on the model

turbine. It must be noted however that the time which is needed for the tunnel mechanism to build up the gust is about 0.4 s. This is relatively large compared to the time scale in the dynamic inflow which according to the results which were obtained from the pitching step measurements on the Tjæreborg turbine (see above) is in the order of 0.1 s.

The (calculated) results for the step on the wind speed on the Tjæreborg turbine however, also showed negligible overshoots. It was found, that the absolute values of the induced velocity (u_i) were hardly modified, despite the change in loading situation and relative axial induction factor (u_i/V_∞) on the turbine. This observation was (to a somewhat smaller extent) found to be true for other turbines as well. It was shown that the change in induced velocity which results from a change in free wind speed is proportional to the local value of $\theta + \alpha_0$, with α_0 the angle of attack at zero lift.

5.1.3 Yawed conditions

In the JOULE I project, a total of four measurement series on the Tjæreborg turbine under yawed conditions have been supplied. The measurement period of every serie was 10 minutes.

Also a total of four measurement series under yawed conditions have been made on the wind tunnel model.

The free stream conditions for the Tjæreborg turbine (free stream wind speed, wind shear coefficient α (best fit from cup anemometers at 5 heights), and turbulence intensity I) are listed in table 5.2. The ambient wind conditions for the four measurement series are more or less comparable but the yaw angle varies between -51° and +54°. A yaw angle of almost zero degrees has been added for reference.

Table 5.2 *Conditions of the Tjæreborg measurements under yawed conditions*

case	ϕ_y [°]	V_∞ [m/s]	α [−]	I [%]	θ [°]	Ω [rpm]
VII.1	32	8.5	0.31	8	0.5	22
VII.2	54	7.8	0.30	2	0.5	22
VII.3	−51	8.3	0.27	11	0.5	22
VII.4	-3	8.6	0.17	very low	0.5	22

The wind direction is measured with a fixed meteorological mast at 2D from the rotor.

Tjæreborg measurements are available of the blade root bending moments at all three blades. Furthermore the yawing moment at the front bearing is measured. However the large negative tilting moment introduces a large error into the yaw moment, due to the inaccuracy of the azimuth reading (30 kNm/(deg. azimuth)). Therefore the yawing and tilting moments which are used in the present project have been obtained from the flatwise moments at blade root from:

$$M_{yaw} = -\sum_{ibl=1}^{ibl=B} M_{flat,ibl}(\phi_{r,ibl}) \cdot \sin(\phi_{r,ibl}) \tag{5.3}$$

$$M_{tilt} = -\sum_{ibl=1}^{ibl=B} M_{flat,ibl}(\phi_{r,ibl}) \cdot \cos(\phi_{r,ibl}) \tag{5.4}$$

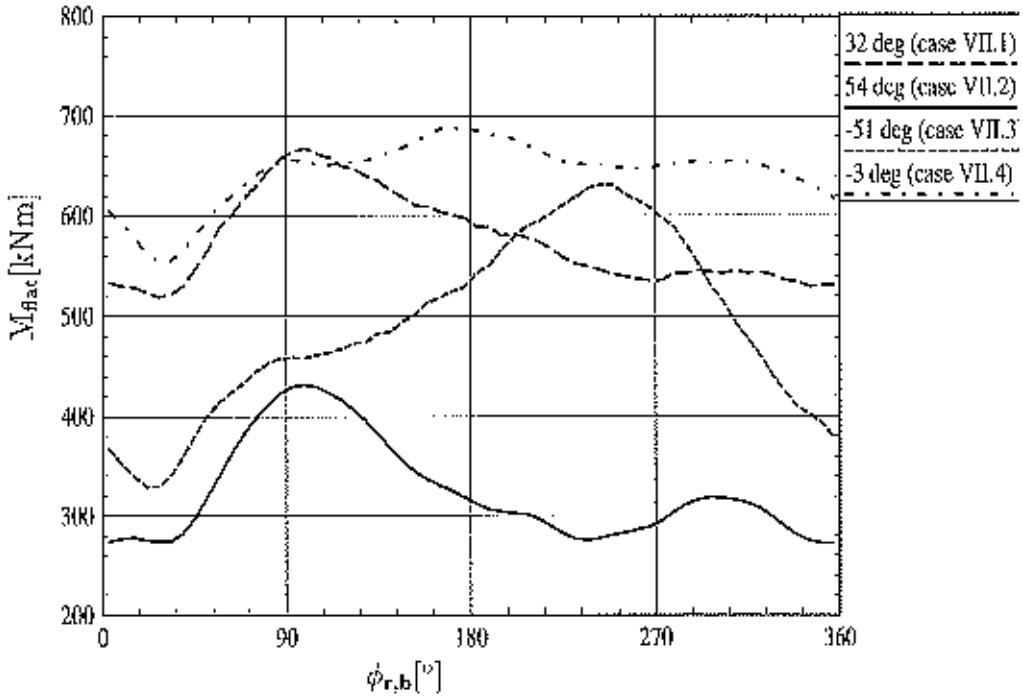

Figure 5.10 *Tjæreborg; Measured flatwise moment at different yaw angles*

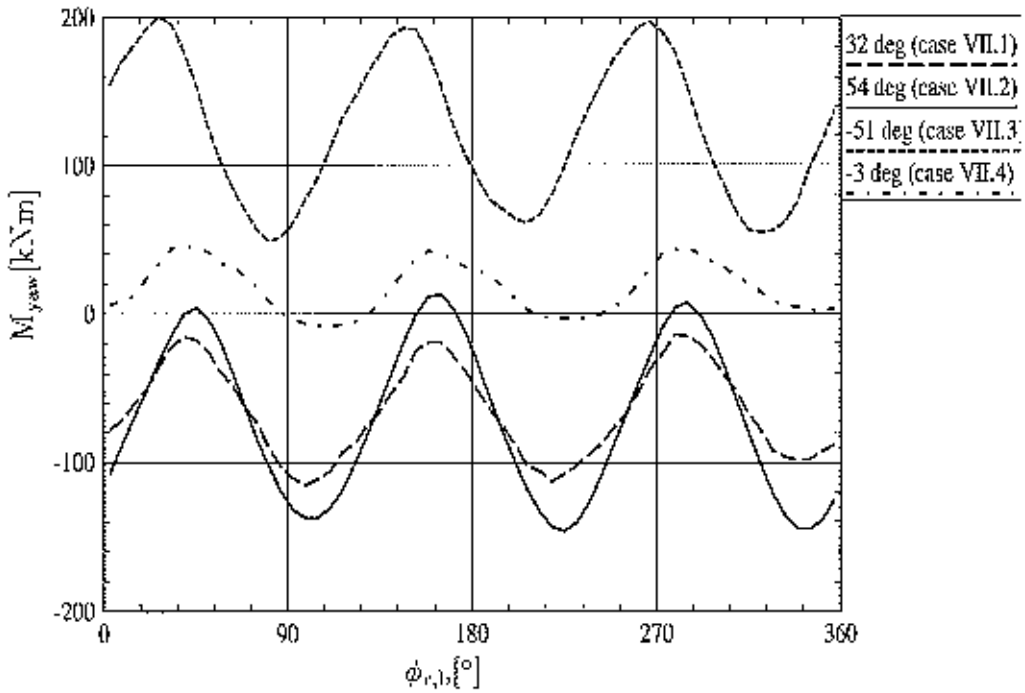

Figure 5.11 *Tjæreborg;Measured yawing moments at different yaw angles*

It must be noted that the yawing and tilting moments as defined above, are not the real moments as experienced on the rotor hub, since the contribution of the blade root forces is not accounted for. However the effects which are of importance for the present project, are expected to be apparent in the yawing and tilting moments from equation 5.3 and 5.4.

The main emphasis in the JOULE I project has been on the azimuthal binned averaged values of the flatwise moment, yawing moment and tilting moment. The

figures 5.10 and 5.11 show the measured results of the binned averaged flatwise and yawing moments on the Tjæreborg turbine, where the yawing moment is derived from the flatwise moment with equation 5.3. The definition of azimuth angle and yaw angle is given in Appendix A. Figure 5.10, shows the measured binned average flatwise moment on the Tjæreborg for different yaw angles. The maximum of the flatwise moment for zero yaw is reached at an azimuth angle of approximately 180 degrees (assuming zero azimuth when the blade points down, see Appendix A). This maximum shifts to azimuth angles of 90 degrees for positive yaw and to 270 degrees for negative yaw. The explanation is given in section 14, where the physical phenomena which play a role in yawed flow are adressed: In the conventional methods, which model yawed conditions, generally only the so called advancing and retreating blade effect is taken into account. This means that the incoming wind velocity vector is decomposed in a component axial and tangential to the rotorplane, where the tangential component is added to the rotational speed. The advancing and retreating blade effect on the blade loads is symmetric around 0 azimuth and of $\cos(\phi_r)$ type, i.e. giving rise to maximum thrust (and flatwise moments) at vertical down position in a homogeneous ambient flow with positive yaw. Such flatwise moments yield negligible (rotor averaged) yawing moments.

In the present project, the influence of the skewed wake geometry on the induced velocity distribution is also taken into account. The proximity to the rotorplane of the vortices in the wake strongly influences the inflow. The trailing tip vorticity is on the average closer to the downwind side of the rotor plane. In the upwind part of the rotorplane the induced velocity is lower than in the downwind part of the rotorplane and consequently the resultant axial velocity in the upwind part is larger than in the downwind part. For positive yaw, this results in maximum thrust when the blade azimuth angle is about 90 degrees and for negative yaw, the maximum thrust is at a blade azimuth angle of about 270 degrees. It must be noted that this shift in phase (which is not predicted with a conventional method) is responsible for the stabilizing yawing moment (negative yawing moment for positive yaw angles and positive yawing moment for negative yaw angles), see figure 5.11, which shows the yawing moments for the Tjæreborg turbine.

In figure 5.12, the measured flatwise moment for the case with large positive yaw angle is compared with the calculated results. Some differences between the calculated results mutually and between the calculated and measured results, are apparent, but most important is that all calculated results predict the maximum flatwise moment at an azimuth angle of about 90 degrees, as is the case in the measurements. As a consequence the resulting yawing moments are stabilising. A conventional model would yield the max-min values at azimuth angles of about 0-180 degrees and a zero yawing moment.

Another interesting observation is that at an azimuth angle of about 270 degrees, there is a 'hump' in the flatwise moment, which is also present in the free wake calculations from Unist and NTUA. Possibly this hump is induced by the root vortex, see section 14: A large amount of vorticity is not only trailed at the tip but also at the root of the blade. The effect of the root vortex is taken into account in the free wake methods, but not in the engineering models. It must be noted, that the hump is not very large and consequently it does not have much importance for practical purposes.

The conditions of the measurement series which have been made in the wind tunnel are summarised in table 5.3.

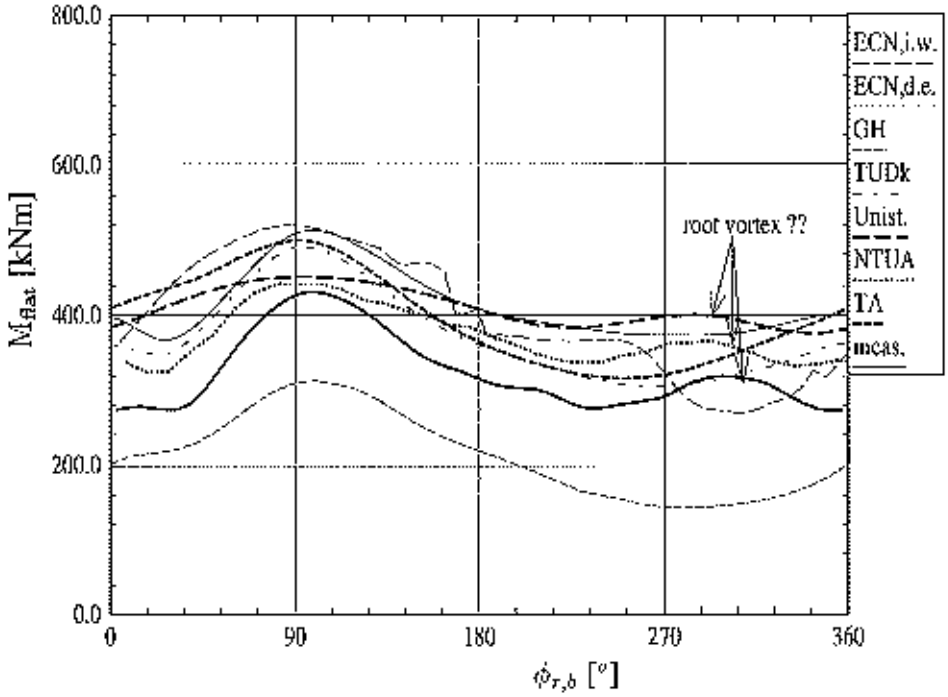

Figure 5.12 *Tjæreborg, Flatwise moment at r = 2.75 m (blade root); ϕ_y = 54°; V = 7.8 m/s (CASE VII.2)*

Table 5.3 *Conditions of the DUT wind tunnel measurements under yawed conditions*

case	ϕ_y [°]	V_∞ [m/s]	θ [°]	Ω [Hz]
VI.1	0	6.0	4.	12
VI.2	10	6.0	4.	12
VI.3	20	6.0	4.	12
VI.4	30	6.0	4.	12

These measurements are made at comparable conditions, the only difference is the yaw angle, which ranges from 0 to 30 degrees with an interval of 10 degrees. Measurements are available of the blade root bending moments at one of the two blades. From the blade root flatwise moment, the yawing and tilting moments have been estimated in a similar way as it was done for the Tjæreborg turbine, see equation 5.3 and 5.4 (The flatwise moment from the second blade was taken equal to the value of the first blade but shifted 180 degrees in blade azimuth angle). The figures 5.13 and 5.14 show the binned averaged flatwise and yawing moments for the wind tunnel model. In the measured flatwise moment on the DUT wind tunnel model, which is given in figure 5.13, the influence of the skewed wake geometry is again clearly visible: For zero yaw angle there is a local maximum at $\phi_{r,b} = 270°$ but for increasing yaw angle, the flatwise moment becomes minimum at this azimuth angle. This leads to a stabilizing yawing moment, see figure 5.14. Figure 5.15 shows the comparison between the calculated and measured flatwise moment of the wind tunnel model for 30 degrees yaw. A reasonable agreement in shape of flatwise moment is found. The larger fluctuations in measured flatwise moment are explained by the non-uniformity of the wind tunnel. All calculated results are on a higher level, due to the fact that no centrifugal stiffening is taken into account in the calculations.

Furthermore the wind tunnel environment delivered interesting flow field measurements under yawed conditions, which cannot be made in the free stream: The horizontal flow velocities are measured in the near wake with a hot wire system, 3 cm (5% R) downstream of the rotor plane at three radial positions (50% R, 70% R and 90% R). The horizontal velocities are measured at several positions at the rotor plane. For one measurement point, the hotwire was fixed at a certain azimuthal and radial position and the blade was passing the hot wire during 10 revolutions. Then the mean value of the measurements was determined. Thereafter the hot wire was moved to another position. By combination of the averaged results at all measurement points, a curve was constructed which gives the wake velocities as function of azimuthal position, see figure 5.16. The measurement is shown together with the calculation from the free wake methods from Unist. and NTUA and with the result as would be obtained from an engineering model.

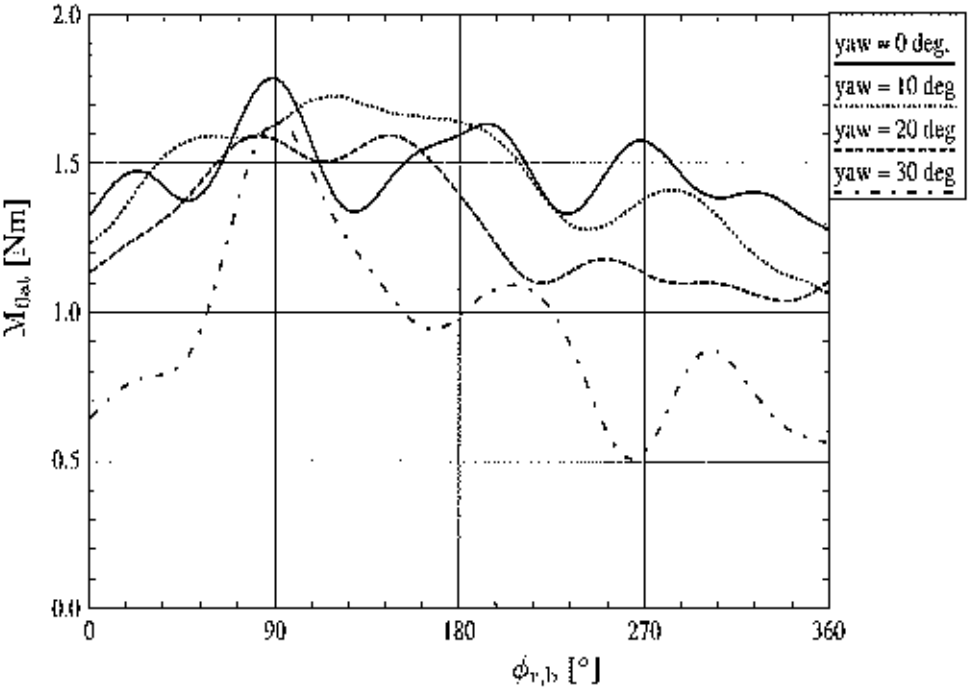

Figure 5.13 *Windtunnel, Flatwise moment at different yaw angles; V = 6.0 m/s (CASE VI)*

It is remarkable to see that in these measurements the total velocity is lower in the upwind part, contrary to the result expected from the engineering methods and described above, that the velocities are larger in the upwind part. The free wake methods reproduce the measurements more accurately. The explanation is that the measured velocity is not that perpendicular to the rotorplane, but the total horizontal velocity which also contains an in-plane, lateral component, induced by the skewed wake, see section 14. This component is taken into account in the free wake methods, but not in the engineering methods. It was not considered worthwhile to implement this component in the engineering methods, because the effect of it on the loads was expected to be limited: The lateral component is expected to be much smaller than the rotational speed and the tangential velocity induced by the root vorticity.

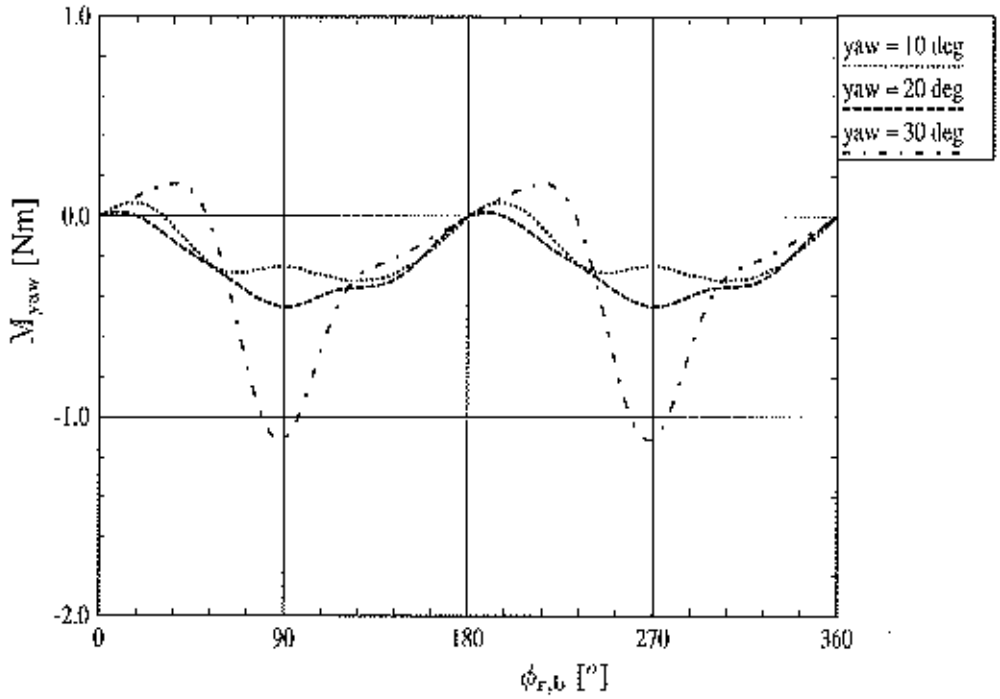

Figure 5.14 *Windtunnel, Yawing moment at different yaw angles; V = 6.0 m/s (CASE VI)*

5.2 Conclusions

In conclusion, the JOULE I project has clearly shown dynamic inflow effects for turbines which are exposed to pitching variations and yawed conditions.

Large overshoots in mechanical loads were found during pitching transients on the Tjæreborg turbine. It must be noted however, that most measurements were taken at an unrealistically high pitching speed and at high loading. In reality, pitching actions will be performed at low loading and with a slower pitching speed, for which the dynamic inflow effects were shown to be more limited.

Both the measurements on the wind tunnel model and the Tjæreborg turbine showed the influence of the skewed wake geometry on the shape and phase of the flatwise moment and consequently the sign of the yawing moment.

The dynamic inflow effects for turbines which are exposed to coherent steps on the wind speed are much smaller. This is due to the negligible change in induced velocity from the step in free stream wind speed.

It is shown that the newly developed engineering methods, predict the dynamic inflow effects much better. However, the presence of the velocity induced in lateral direction, which was found in the wind tunnel flow field measurements under yawed conditions, and the root vorticity effects which are predicted with the free wake methods, are not taken into account in the engineering methods, because they were expected to be of limited practical importance.

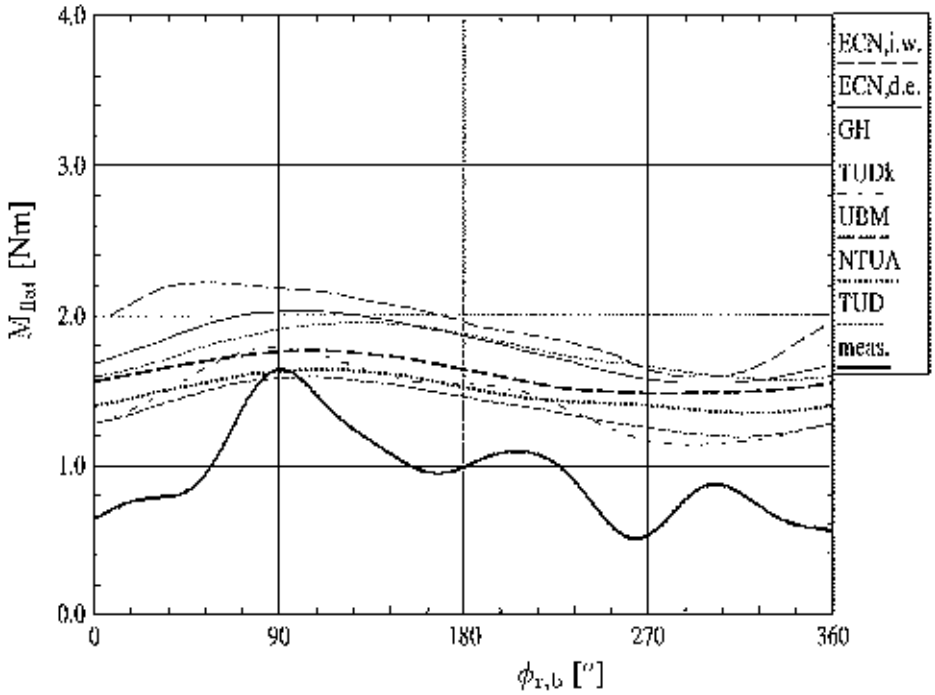

Figure 5.15 *Windtunnel, Calculated and measured flatwise moment; ϕ_y = 30°; V = 6.0 m/s (CASE VI.4)*

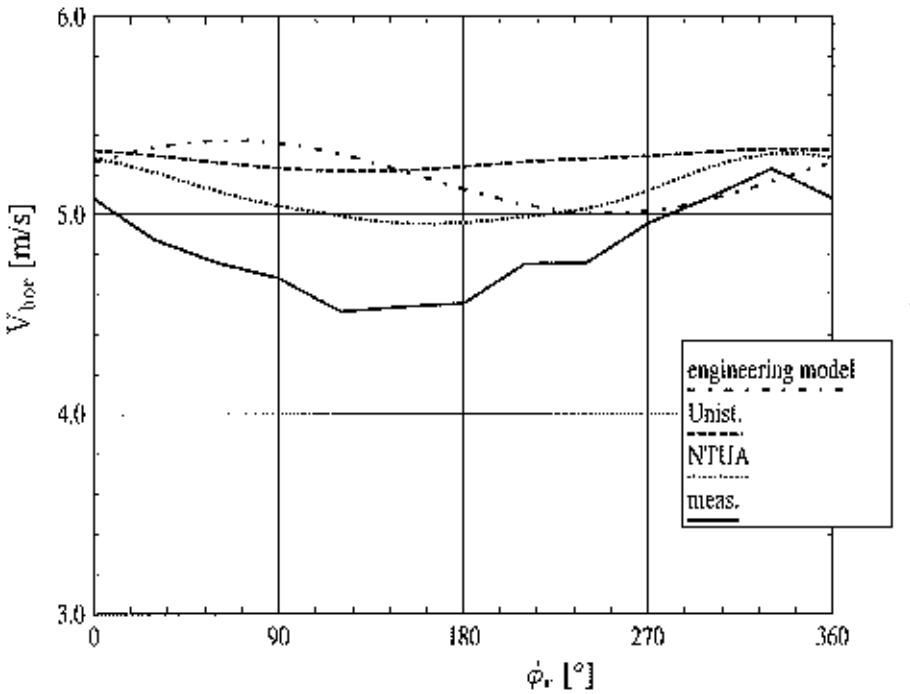

Figure 5.16 *Windtunnel, Horizontal velocity at 70% span; ϕ_y = 30°; V = 6.0 m/s*

6. CHARACTERISTICS OF THE TURBINES

Both full scale measurements and wind tunnel measurement are used in the project. The present chapter summarises the characteristics of the facilities used, viz. the Uniwex wind turbine, the WPS-30 wind turbine, the Howden Richborough wind turbine and the DUT open jet wind tunnel with model turbine.

The Uniwex turbine was used for measurements of pitching transients and for measurements in yawed flow conditions, (yaw angles between -50 degrees and +50 degrees approximately).

The WPS-30 turbine was used for measurements of pitching transients.

The Howden Richborough turbine was used for measurements of partial span pitching transients.

In the present project, the DUT open jet wind tunnel has been used for measurements of pitching transients.

For the full scale facilities, mechanical loads have been measured only. In the wind tunnel, the wake flow field has also been recorded.

The global characteristics of these turbines are listed in the following subsections. Detailed data, are given in Appendix K, Appendix L, Appendix M and Appendix N. These data have been used by the participants to compose the aeroelastic model of the turbines, and should be sufficient for any party who would like to compare his method with the results as reported here. The aeroelastic turbine data can be obtained from the coordinator on floppy disc, upon request.

6.1 Uniwex turbine

Diameter	16 m
Start of aerodynamic part of blade	r = 1.6 m
Hub height	14.625 m
No. of blades	2
Tilt angle	0 °
Cone angle	0 °
Ω	variable, but fixed for the present project

The blade eigenfrequencies (at 70 rpm) are :

Flap	4.4 Hz
Lead-lag	6.2 Hz

Tower bending eigenfrequency: 2.55 Hz

The blade bending moment in flapwise (perpendicular to rotorplane) direction

is measured at r = 1.0 m. The blade bending moment in flatwise (perpendicular to local chord) direction is measured at r = 4.0 m and r = 5.6 m.

The flow field is measured with a (fixed) meteorological mast with cup anemometers and wind vanes at 3 different heights (7m, 10m and 16m). In all calculational cases, this meteorological mast was upstream of the turbine.

It is of importance to note that due to the fact that the twist which was supplied by Unist. had a tip value different from zero, a pitch angle (θ) zero for the Uniwex turbine, does not imply that the tip chord is in the rotor plane, as is the case for the other turbines in the project.

6.2 Wind tunnel model

Diameter	1.2 m
Number of blades	2
Root cut out	30%
Aerofoil sections	NACA 0012
chord	0.08 m (no taper)
total twist	6 degrees from $0.3 < r/R < 0.9$ outer 10% of blade: untwisted
Rotor speed	.25 - 16 Hz ($\pm$ 0.05 Hz)

OPEN-JET WIND TUNNEL data:

outlet diameter	2.24 m
maximum wind speed	14.5 m/s
turbulence intensity	0.8%
uniformity over section	within 2.5%

Measured quantities:

- Flat and lead lag blade root bending moments at r = 0.134 m radial position (at different blades)
- Axial force;
- Azimuth angle and rotor speed;
- Undisturbed tunnel wind velocity by means of pitot tube and Betz manometer;
- Additional wake flow velocities are measured with a hot wire system at one radius downstream of the model turbine.

6.3 WPS-30 turbine

Diameter	30.1 m
Start of aerodynamic part of blade	r = 3.0 m
Hub height	35 m
No. of blades	3
Tilt angle	5.5 °
Cone angle	0 °
V_{rated}	14 m/s
P_{rated}	300 kW
Ω	variable between 30 and 44 rpm,fixed for the present project
Generator	synchronous with a dc link

The blade eigenfrequencies are (at 30 rpm):

Flap	3.6 Hz
Lead-lag	6.0 Hz

Tower bending eigenfrequency: 1 Hz

Blade bending moments (flatwise and edgewise) are measured at r = 3.5 m and r = 8.5 m. Furthermore the torque on the low speed shaft is measured.

The flow field is measured with a (mobile) meteorological mast with five 3D propellor anemometers which are placed 1D upstream of the turbine.

6.4 Howden Richborough turbine

Diameter	55 m
Start of aerodynamic part of blade	r = 4.25 m
Hub height	45 m
No. of blades	3
Tilt angle	0 °
Cone angle	0 °
P_{rated}	1000 kW
Ω	24.5 rpm

The blade eigenfrequencies are (at 24.5 rpm):

Flap	1.415 Hz
Lead-lag	2.565 P

7. SHORT DESCRIPTION OF MODELS FOR THE FULL SPAN PITCH CASES

7.1 Introduction

In this chapter the short overview of the different methods which have been used by the various participants to model the full span pitching cases is copied from [1].

In this introduction, a physical description of the phenomena to be modelled will be given.

In the equilibrium situation, the axial flow velocity (inflow) in the rotor plane depends on the wind speed and on the degree of loading (axial force) of the turbine. For instance, for a turbine with zero loading, the speed in the rotor plane is equal to the wind speed, while an operating, loaded wind turbine slows down the wind speed to a lower value. The difference between (the axial component of) the wind speed and the axial flow velocity in the rotor plane is usually called the 'induced' velocity, the velocity induced by the presence of the turbine. Figure 7.1 shows this principle for a non loaded and a loaded wind turbine. When the load situations changes, the change in the induced velocity will lag behind, since an appreciable amount of air must be accelerated or decelerated.

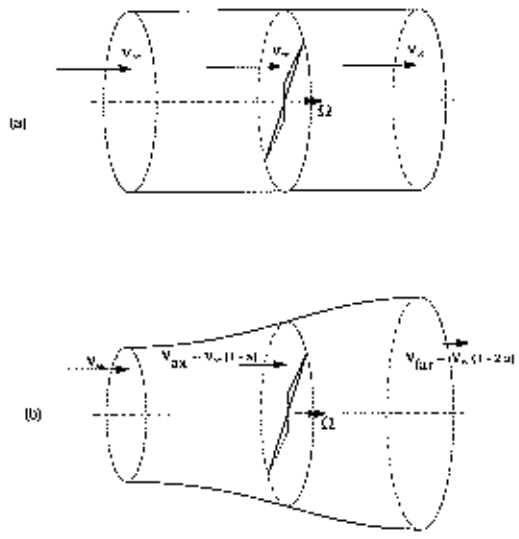

Figure 7.1 *Wind turbine with and without loading*

In the actual operation of the wind turbine, its load situation is changing continuously, either because of wind speed fluctuations or through blade angle variations (pitch control). Nevertheless, most of the operational computer codes for the prediction of these loads and of the dynamic behaviour of turbines, make use of quasi steady aerodynamic models, assuming at any instant in time an equilibrium

between the load situation and the induced velocity. Therefore, differences may occur which can be attributed to unsteadiness and the time lag in the adjustment in the induced velocity during pitching transients.

This phenomenon can be described by taking into account the unsteady formation of the rotor wake, and its effect on the 'inflow' into the rotor plane of the turbine. This is done by the so called free vortex wake models that are able to calculate the wake formation and subsequent development, and its feedback on the inflow in the rotorplane. In the project such methods are contributed by the University of Stuttgart and the National Technical University of Athens. However, these methods require considerably more computer time than the simpler aerodynamic models. For that reason, they are not usually incorporated in the aeroelastic programs (calculating loads as the combined result of aerodynamics and structural dynamics) used by wind turbine designers. Moreover, these methods are of a nature that limits their validity to attached flow around the blades and to a few diameters downstream of the turbine (no viscous effects are accounted for). In the project, this type of models is used to obtain essential information and physical insight into the most important phenomena, to be fed into the engineering methods.

From a more global point of view, the blade element momentum relations which equate instantaneous forces (on the blade) to the momentum difference in upstream and downstream sections, can be converted in a non-equilibrium relation by adding a time lag term. This is the approach taken in the engineering models that are developed and used within this project. This changes the algebraic blade element momentum relations into ordinary differential equations in time, which are easily implemented in the existing aeroelastic codes. In fact, in these codes a set of differential equations is already solved in the time domain, for the structural degrees of freedom.

7.2 Models used in the project

In the project seven models (including the free wake models) are applied. These will shortly be described below. For detailed model descriptions reference is made to [1].

ECN, cylindrical wake model
The induced velocities in both axial and tangential direction are calculated with a cylindrical vortex sheet model. A constant bound vortex strength along the blade is assumed. The vortex distribution on the cylindrical wake is obtained by the time history of the trailed tip-vorticity which is related to the axial force on the blade. With the Biot-Savart law the induced velocities can then be found. It is assumed that the wake extends up to three rotor diameters downstream. Inputs that may be semi-empirically adjusted are the axial convection velocity and the effective diameter of the cylindrical wake. A detailed description of the model is given in Appendix I.

In the present project, the model has only been used to reproduce a few cases, because it was developed to deliver additional insights into dynamic inflow phenomena. For design purposes the second ECN model is applied:

ECN,differential equation

The induced velocity in axial direction is calculated with the blade element - momentum equation with the addition of a time derivative of the induced velocity:

$$4Rf_n(\frac{r}{R})\frac{d}{dt}(u_i) + 4u_i(V - u_i) = \sigma V_{eff}^2 c_n \tag{7.1}$$

The value of the time constant is derived from the equations for the cylindrical wake mentioned above (ECN, i.w.).

$$f_n(\frac{r}{R}) = 2\pi / \int_n^{2\pi} \frac{[1 - r/R\cos\phi_r]}{[1 + (r/R)^2 - 2r/R\cos\phi_r]^{3/2}} d\phi_r \tag{7.2}$$

In a similar way the tangential induced velocity is calculated from the tangential momentum equation with time constant r/R.

The DUT model

Within the Institute for Wind Energy of T.U. Delft an aerodynamic model has been developed a number of years ago based upon the asymptotic acceleration potential theory [10] , [11]. Under the assumption of incompressible, inviscid and irrotational flow, in situations where the velocity perturbations are small with respect to the undisturbed value, it can be shown that the pressure perturbation in the complete flow field is given by a Laplace equation:

$$\nabla^2 p = \frac{\partial^2 p}{\partial x^2} + \frac{\partial^2 p}{\partial y^2} + \frac{\partial^2 p}{\partial z^2} = 0 \tag{7.3}$$

The pressure perturbation p then acts as an acceleration potential function. Integration of the accelerations experienced by particles of air, which travel from far upstream to the rotor blade, determines the velocities in the rotor plane. With these velocities the aerodynamic loads can be calculated.

In the model the rotor blades are represented as discrete surfaces on which a pressure discontinuity is present. The model implies the presence of spanwise and chordwise pressure distributions, which are composed of analytical asymptotic solutions for the Laplace equation. This makes the approach equivalent to a lifting surface model. A similar approach for the determination of loads on helicopter blades was described by Van Holten [12]. In the first order approximation used for the present purpose, the chordwise pressure distribution is restricted to a flat plate type analogon.

Asymptotic expansion techniques are often used in finding solutions of Laplace equations. The lifting line approach is such an example: Often the span of a lifting surface is large with respect to the chord (e.g. an aircraft wing or a wind turbine rotor blade). At some distance of such a surface (in the far field) the experienced accelerations will be equivalent to those felt by a line on which the load is concentrated. So in this area the wing can be modelled with a pressure dipole line. Close to the surface the experienced accelerations will be dominated by the chordwise load distribution. So in the near field the experienced accelerations will be almost two dimensional, and can be modelled with two dimensional pressure distributions.

Application of asymptotic expansion techniques to the pressure distribution representing the rotor blade eventually leads to:

$$\frac{p}{0.5\rho V^2} = -\frac{1}{\pi}\frac{l(y,t)}{0.5\rho V^2 c(y)}\frac{\sin(\Phi)}{(\cosh\eta+\cos(\Phi)} + \frac{1}{2\pi}\frac{l(y,t)}{0.5\rho V^2 c(y)}\frac{c(y)}{r_b}\sin(\chi) +$$

$$\frac{1}{\pi}\sum_{n=1}^{\infty} A_n(t) P_n^1(\cos\theta) Q_n^1(\cosh\nu)\sin\chi \qquad (7.4)$$

In 7.4 the expression c(y) yields the chord distribution.

The first expression on the right hand side of equation 7.4 is the near field term written in local elliptical coordinates Φ and η. The third expression is the far field term, written in prolate spheroidal coordinates θ, ν and χ; and the middle expression in the right hand side is the common field expression written in circular cylinder coordinates y , r_b and χ. The P_n^1 and Q_n^1 functions represent associate Legendre functions of the first and second kind. Legendre functions are the natural solutions for problems written in prolate spheroidal coordinates. In equation 7.4 it can be seen that close to the blade the common field expression exhibits a singular behaviour (caused by r_b^{-1}). This behaviour is also found in the far field term (when the Q_n^1 term is evaluated), but with the opposite sign. Thus the total expression does not have this essential singularity.
In expression 7.4 the function l(y ,t) is used. This is the liftdistribution over the blade. It can also be expressed in terms of associate Legendre functions of the first kind:

$$l(\frac{y}{b/2},t) = 1/2\rho V^2 b\sqrt{1-\frac{y}{b/2}^2}\sum_{n=1}^{\infty} A_n(t) P_n^1(\frac{y}{b/2}) \qquad (7.5)$$

The coefficients $A_n(t)$ are determined by application of the tangential flow condition using a collocation point method.
In its simplest implementation (code PREDICHAT 1) an iterative procedure is developed for the calculation of the stationary coefficients A_n. It starts from an assumed straight, unperturbed path, which is travelled by the particles of air with an imposed constant speed. For the speed the value 0.6667*V is used, the optimum value in the rotorplane determined by axial momentum theory. The accelerations experienced during the travel are integrated in order to obtain the velocities at the collocation points. This yields a first guess of the stationary coefficients A_n.
With the resulting pressure field the perturbed axial velocities of the particles travelling to the collocation points can be calculated. Within the code PREDICHAT 1 the velocity is kept constant along the straight unperturbed path, although its value is collocation point dependent. In repeating this iterative procedure the ultimate stationary coefficients are determined. In a more elaborated version (PREDICHAT 2) the option of a perturbed path with time dependent velocity can be chosen.
The induced angle is determined in the present method by integration of the common field and the far field terms (2nd and 3th term of expression 7.4).

The time dependent (dynamic inflow) solutions are obtained according to the following procedure:
First a stationary calculation is carried out using PREDICHAT. This calculation

uses the initial values of the relevant parameters (such as pitch angle and wind speed at "t = 0").
With the now well determined stationary pressure field the unsteady paths of the particles (and their time and position dependent velocities) are calculated using a step by step variation procedure. Every next step the whole process of determination of the accelerations (now time dependent), the velocities and the paths is repeated, thus calculating the dynamic inflow velocities in the rotor plane. The latter process is equivalent to a vortex wake calculation with a dynamically varying wake (a process called dynamic wake adaptation). The code in which this calculation is implemented is designated PREDICDYN.

The GH model
The axial induction is calculated using a method based on the Pitt and Peters model [3] but GH applies the method to each blade element assuming independent annuli. This is consistent with the combined blade element and momentum method used in the GH aeroelastic code BLADED. The Pitt and Peters model was originally developed in terms of induction factors. GH used this approach initially but later in the project developed the model to work in terms of induced velocity.

The TUDk model
The induced velocities in axial direction are calculated with the blade element - momentum equations with the addition of a time derivative of the induced velocity. This is similar to "ECN, d.e.". TUDk however uses two differential equations. These have the following form:

$$y + \tau_1 \cdot \frac{dy}{dt} = x + k \cdot \tau_1 \cdot \frac{dx}{dt}$$
$$z + \tau_2 \cdot \frac{dz}{dt} = y$$

with $k = 0.6$ and:

$$\tau_1 = \frac{1.1}{(1 - 1.3a)} \cdot \frac{R}{V}$$
$$\tau_2 = [0.39 - 0.26(\frac{r}{R})^2] \cdot \tau_1$$

This amounts to one short and one longer time scale for the decay. The time constants follow from an actuator disk-vortex ring program which includes the effect of wake expansion.

The Unist. method
The Unist. free wake method is based on the solution of the Laplace equation. The rotor blades are covered with panels having constant doublet strength. Using the equivalence of a doublet panel and a vortex ring the induced velocities are calculated by Biot-Savart law where the vortex strength is gained by doublet differences. The kinematic boundary condition on the blade and the Kutta condition are fulfilled automatically by the numerical method. Due to the free stream velocity, rotation and induced velocities at the blades, points from the separation edges move downstream and build up the panels of the free wake which is deformed in such a way that the forces on the wake vanish. The results of the method are:
- Doublet distribution along the blade,

- Wake geometry,
- Representation of the flow field.

The NTUA model

The flow around a horizontal axis wind turbine is an unsteady three-dimensional vortical flow with moving boundaries. More specifically:

- The flow is three-dimensional because wind turbines operate in the atmospheric boundary layer. For the same reason the flow is also unsteady (periodic) even if the inflow is assumed steady in time (Unsteadiness can also originate from transient operational controls).
- The flow is vortical (or rotational) due to the spatially distributed vorticity. On the blades bound vorticity appears as a result of their shape. Due to the three-dimensional character of the flow and according to Kelvin's theorem vorticity will be shed in the undisturbed flow.

For detailed computations of vortical flows of this kind, Vortex Methods (VM) seem to be a good choice, mainly because of their grid-free structure. In fact vortex methods were constructed so as to approximate numerically complex flows at low computational cost.

Within this context, a free-wake aerodynamic model has been defined and incorporated in a computational environment by the name GENUVP (GENeral Unsteady Vortex Particle code). GENUVP is a time-marching code based on a consistent combination of the Boundary Element Method (BEM) and the Vortex Particle Method (VPM). The BEM is used to reproduce numerically the irrotational part of the velocity field, i.e. the flow induced by the blades. This is accomplished by distributing sources and/or dipoles on the solid surfaces of the flow. The boundary conditions of the flow, determine the intensities of these distributions. On the other hand, the VPM is used to simulate the generation and evolution of the free-vorticity contained in the wakes of the blades. Particularly, the vorticity shed along the edges of the blades, is locally integrated and assigned to point vortices (or equivalently to fluid particles carrying vorticity). Next the evolution of these vortex particles is followed by integrating the vorticity transport equations in Lagrangian coordinates.

During the progress of the present project but within another JOULE project, entitled "Development of a new generation of design tools for horizontal axis wind turbines" (JOU2-CT92-0113), GENUVP was improved and completed. First, the tower was included as a non-lifting body represented by a distribution of sources over its surface. Second GENUVP was coupled with a beam-type structural model, to give a non-linear aeroelastic numerical model. The full model was used in the cases of yawed operation where the aeroelastic coupling plays a dominant role.

Some additional comments to the model description given in [1], can be found in Appendix J.

7.2.1 Qualitative discussion of the differences between models

The 'engineering models' have in common that they are adaptations of the blade element momentum (bem) method. In case of steady circumstances, they will reduce to the steady blade element momentum theory. There are however some differences in the way the bem expressions are adapted, which will be discussed here.

The ECN d.e. and the TUDk models add time derivative terms of the dimensional quantity u_i. Physically this is the correct way, since the time varying wake vorticity changes the induced velocity. In the original Pitt and Peters model (see chapter 6 of [1]), the time derivative is of a nondimensional form of u_i, where the tip speed Ωr is used to non-dimensionalise. In the original GH implementation of the Pitt and Peters model, a time derivative of the nondimensional induced velocity factor 'a' (i.e. u_i divided by the wind speed V_∞) is used. All these methods would be equivalent if V_∞ or Ωr were constant. In wind turbine applications, Ωr is frequently constant (constant rpm operation) but of course the wind speed never is. The GH model was changed during the course of the project so that the induced velocity is calculated directly. Then, there is very little difference between the approaches from ECN, GH and TUDk.

All of the 'engineering methods' include dependence of the time constants on rotor size but approach the radial dependence of the time constants in different ways. The GH implementation of the Pitt and Peters model, because it works at the annulus level, has a radial dependence which has an inverse relationship with radial position. The ECN d.e. model uses a physical argument which comes directly from the cylindrical wake model which causes the time constant to reduce near the tip. This is related to the dominant behaviour of the tip vortex in determining the inflow distribution. The TUDk model has a similar radial dependence of the shorter of the two time scales applied. The absolute magnitude of the time constants is not so easy to estimate. Some estimates will be given in the chapters which report the pitching step measurements.

A final difference in implementation is between the TUDk model on one side and the ECN d.e. and GH models on the other side. The first model has a set of two equations describing the changes of the induced velocity in time, modelling basically two time scales: one for the initial phase (e.g. directly following the pitch step) and one for the remaining phase. This mimics the behaviour observed in numerical results from a vortex ring wake model.

The remaining models used in the project are the acceleration potential model of the DUT and the free vortex wake models of the Unist. and the NTUA. All three methods are basically flow field solvers for inviscid flow. In the near field of the flow about the rotor blades, this restricts the applicability to attached flow. In the far field (the global rotor wake) the applicability is restricted to the region where viscous diffusion and/or dissipation of vorticity is not important. This is most likely true for that part of the wake which is important for the induced velocity in the rotor plane, i.e. a few rotor diameters behind the rotor plane.

The DUT model is linearized in the sense that a small perturbation equation is solved, the other two solve the complete equations, making use of surface singularity distributions on the blade (vortex lattice) and vorticity distributions in the wake. The difference between the Unist. and NTUA models is mainly in the wake resolution technique applied. The Unist. uses vortex filaments as a natural extension of the blade vortex lattices, while the NTUA uses a vortex particle representation in the wake. The reader is referred to the appendices O and Q of [1] for the details of the implementation.

One important aspect of the free vortex wake models is the desingularisation of the vortex particles or filaments. This has been the subject of a more detailed numerical study which is discussed in the next subchapter. In conclusion no fundamental differences are present between the NTUA and Unist. models.

7.2.2 Numerical study of convergence and desingularisation of the free vortex wake models

The free vortex wake models are based on an exact formulation of the inviscid flow equations. This means that these models can in principle be very accurate, on condition that there are no important viscous effects in the real flow. The long experience with non-viscous flow models (both analytical as well as numerical models) has provided sufficient background to know the limits of application of such models. In the dynamic inflow project there are no special conditions encountered which would give rise to more than the usual caution in this respect.

The next question is, whether the actual numerical implementation chosen could introduce errors of such magnitude that appreciable differences with the "exact" inviscid flow occurs.

In this respect the discretisation procedure warrants special attention. For practical purposes it is obviously necessary to discretise the continuous formulation of the exact theory. In the present case the continuous vortex distributions are discretised into either vortex lattices or into a distribution of discrete vortex particles.

Such a discretisation artificially introduces singularities in the description of the flow field. These singularities take the form of points or lines where the velocities become infinite, which is obviously a large departure from the actual physical flow.

Nevertheless, in a case where the position of the singularities is fixed in space (linearized theory) or is prescribed beforehand as a function of time on the basis of experiments ("prescribed wake methods"), it can be shown that the correct inviscid limit is approached when the number of discrete vortex elements is increased indefinitely.

One of the purposes of the "free wake" analyses used in the dynamic inflow project is, to be able to determine by computation the shape and configuration of the free vortex sheets. The position of the singularities in the wake is in that case not fixed, but is instead determined during the computation by letting the vortex elements float freely through the field in such a way that a "force free" condition is satisfied, as it should be.

In the case of freely convecting vortex elements ("free wake") there may occur a computational stability problem due to the very irregular flow field associated with the discretised singularities.

For this reason artificial desingularisation (or: "regularization") is used in both free-wake methods used in the dynamic inflow project. This is done by the introduction of a "cut-off" length: close to the singular points a regular flow field is substituted in place of the almost singular flow field near the discrete singularities. Very roughly speaking, one can compare this artifice physically with a kind of viscous vortex core.

Although the mathematical form of the desingularisation and the numerical constants chosen are different between the vortex lattice method and the vortex particle method, in both these methods the goal has been achieved that numerical instability is avoided.

What has to be investigated next is, whether the convergence characteristics are still maintained, i.e. whether the numerical solution despite the regularization still converges to the exact inviscid solution when the number of discrete singularities

increases indefinitely.

A simple testcase has been used to obtain some insight in this question. The testcase consisted of a two-dimensional strip on which vorticity is continuously distributed in such a way that the self induction is constant along the strip.

Although the testcase is mathematically very simple and possesses an exact solution in closed form, in some respects it is a very a demanding testcase. What is in fact tested is, how accurately a numerical calculation will predict the free convection of vorticity under rather difficult circumstances, viz. in the edge region of the free vortex sheets in the wake.

Some of the test results are shown in the figures 7.2 and 7.3.

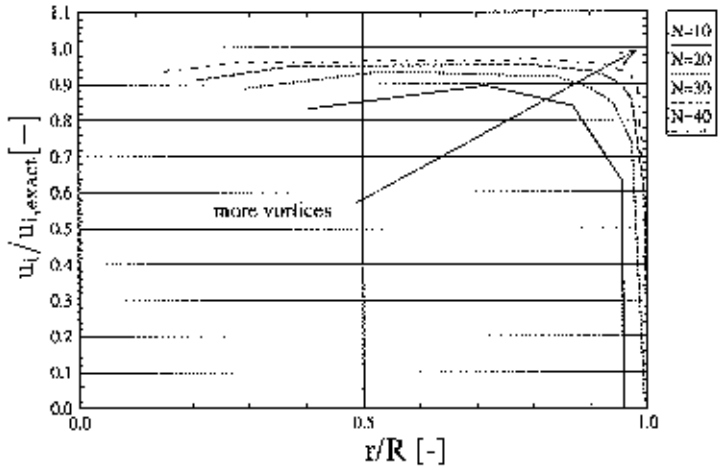

Figure 7.2 *Influence of discretisation, 2D vortex strip*

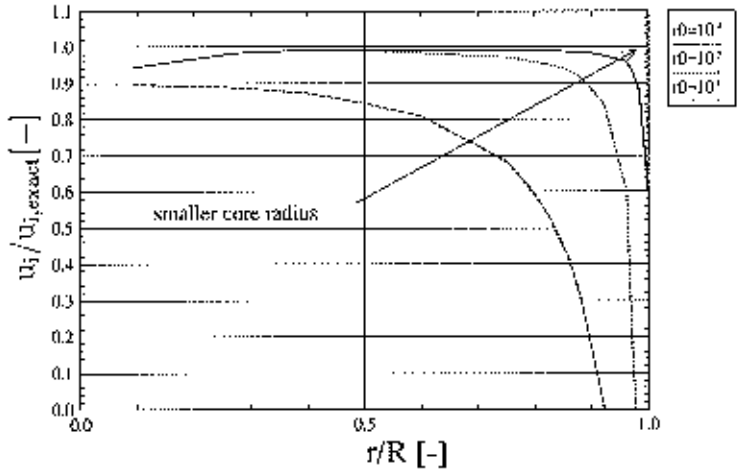

Figure 7.3 *Influence of core radius, 2D vortex strip, N=80*

Figure 7.2 shows first of all the influence of the number of discrete vortex elements (N). It is seen that the numerical results converge towards the exact solution. When the number of discrete vortices is chosen at N ≈ 80, the difference with the exact result is probably negligible for all practical purposes.

Figure 7.3 shows the influence of the "cut-off length (r0)". It is found that one should be careful with the regularization procedure, because the exact result is only recovered when small cut-off lengths are used.

One may conclude that a free wake analysis will be stable as well as convergent, as long as the number of discrete vortices and cut-off length are carefully chosen, in a mutually consistent way. In both the free wake methods of the project this has been done, by choosing only certain combinations of grid size, time step and cut-of length. When the grid size and time steps are decreased, at the same time the cut-off lengths are made smaller.

The finally remaining question is then, how accurate the numerical free wake analyses are in the case of a practical choice of grid size and time step.

In practice the number of discrete vortex elements is necessarily much smaller (relatively) than in the testcase considered above. This would mean that the finer details of the flow near the edges of vortex sheets, and the details of the rolling up of vortex sheets cannot be represented very accurately by the free wake analyses.

In the remaining parts of the flow field where the velocity gradients are much smaller, the situation will be more favourable.

A test that has been done for both the numerical methods was, how sensitive the resulting load distributions on the blades of the rotor are with respect to grid size and time step. In both methods the grid size was chosen such that a refinement of the grid size did not add additional accuracy to these load distributions.

Loads however constitute a relatively insensitive criterion. It is well known that the vortex configuration often does not influence very critically the resulting loads. This is the very reason why linearized methods where the vortex sheets are assumed to lie in flat planes without deformations by self induction effects, are often very successful.

In conclusion it can be said that in those flow regions where the deformations of the free vortex sheets are really of importance, and for which free wake methods are essentially meant, the grid size would probably have to be made much smaller than is practically feasible at present. However, such refinements would not make much sense as long as there is a lack of experimental data to validate the numerical methods. What would be needed first of all are flow field measurements, revealing considerable detail of the kinematics of the wake deformations and the formation of "tip vortices" of rotors.

8. AXIAL SYMMETRIC CASES, WPS-30

8.1 Available measurements

In this section the measurement series are described which have been taken on the WPS-30 turbine at pitching steps and which have been used to further validate the model under axisymmetric conditions.

8.1.1 Measurement accuracy

In the present project, measurements of wind conditions, pitch angle and flatwise moments at two different radial stations on the WPS-30 turbine have been used.

It is known from [13] and [14] that the measurements of the flatwise moments suffer from a large unknown zero-drift, but that the dynamic part of the loads is expected to be reliable. Also the measurements of the pitch angle, and the wind conditions are believed to be very accurate.

8.1.2 Discussion of pitching step measurements (case WII)

The figures 8.2 and 8.4 show the measured flapwise moments for a step on the pitch angle going up and a step going down. The corresponding pitch angle time series are presented in the figures 8.1 and 8.3.

Every time series is averaged over about 25 separate measurement series, similar to the procedure which was followed for the Tjæreborg turbine in the JOULE I project, see section 5.1. However data from one blade only, are available.

The flatwise moments were measured at two radial positions (r = 3.5 m, 23% span and r = 8.5 m, 57 % span). The pitching steps are from -2.25 to -0.25 degrees. The wind speed is about 9 m/s.

In addition to the flatwise moment, the rotor shaft torque has been measured as well. Although the WPS-30 turbine is commonly operated in variable speed mode, a constant rotor speed of 36 rpm was applied for the present measurements. Nevertheless, the change in applied led to a small acceleration or deceleration of the rotor, which diminishes the overshoots in the rotor shaft torque from dynamic inflow. This is the reason why the rotor shaft torque measurements are not used.

In table 8.1, the conditions of the measurements are summarised with the identification of the cases. The wind speed is the average value for the case, θ_1 is the initial blade pitch angle, θ_2 the one after the pitch step. The value of Δt gives the time in seconds used for the pitching change. Also indicated in this table are calculated values of the equilibrium induction factors a_1 and a_2 at 70 % span, to give an indication of the loading situation.

The figures 8.2 and (more clearly), 8.4 show that the pitch changes result in overshoots, similar to the ones which were found in the JOULE I project on the Tjæreborg turbine (See section 5). However, the overshoots are considerably smaller than those for the Tjæreborg turbine. This is mainly explained by the fact that the time scale in the dynamic inflow process decreases with decreasing rotor diameter (see also section 5.1). Since the pitching speeds in the WPS-30 experiments were similar to the pitching speeds in the Tjæreborg measurements, the overshoots in the loads appear smaller for this smaller scale machines.

Table 8.1 *Conditions of the WPS-30 pitching step measurements*

case	λ [-]	V_∞ [m/s]	θ_1 [°]	θ_2 [°]	Δt [s]	a_1 [-]	a_2 [-]	Ω [rpm]
WII_up	6.35	8.93	−2.25	0.25	0.5	0.32	0.25	36
WII_down	6.35	8.93	−0.25	−2.25	0.6	0.25	0.32	36

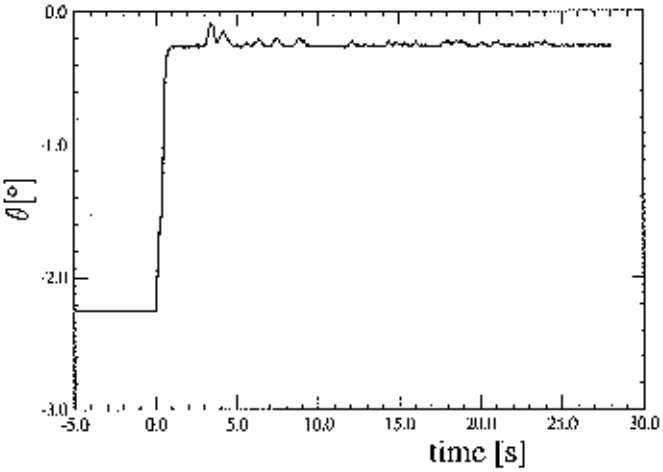

Figure 8.1 *WPS-30; Measured pitch angle for case WII_up* V_∞ *= 8.93 m/s*

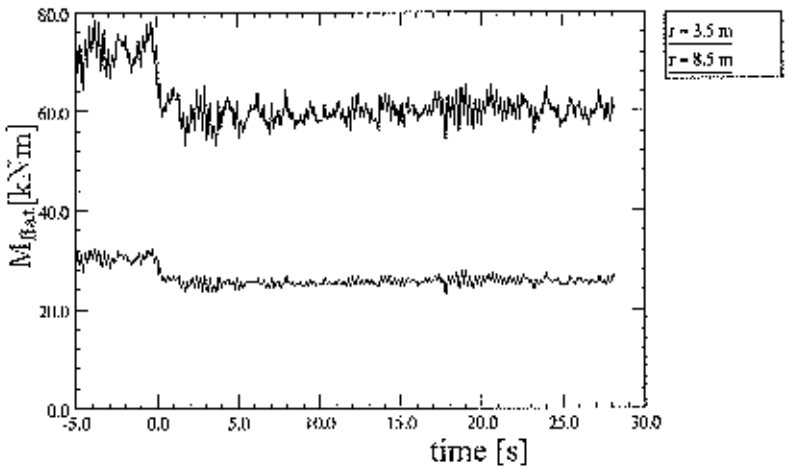

Figure 8.2 *WPS-30; Measured flat moment at blade root for step on the pitch angle going up, case WII_up*

8.2 Definition of calculation cases

Two cases on the WPS-30 turbine were defined. The first one was denoted by case WI. This preliminary case was defined before the measurements from section 8.1.2 had become available. Case WI was subdivided into two subcases case WI.1 and WI.2. After the measurements had become available, a new case (case WII) was defined in agreement with the measurement conditions. It turned out that the definition of case WI.1 was very close to the measurement conditions of case WII and therefore no updated results were supplied for case WI.1 since then. This is

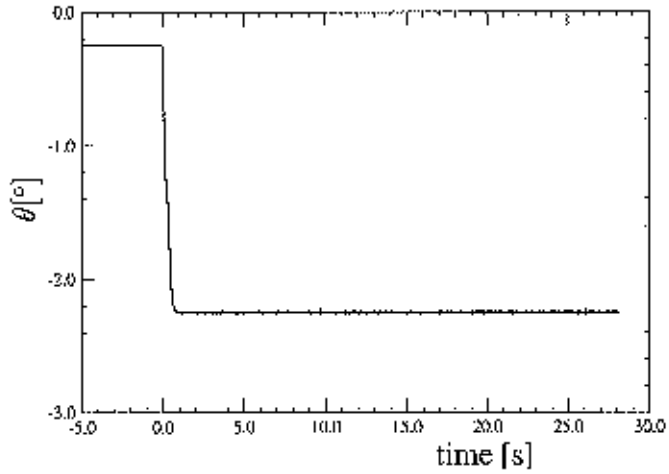

Figure 8.3 *WPS-30; Measured pitch angle for case WII_down V_∞ = 8.93 m/s*

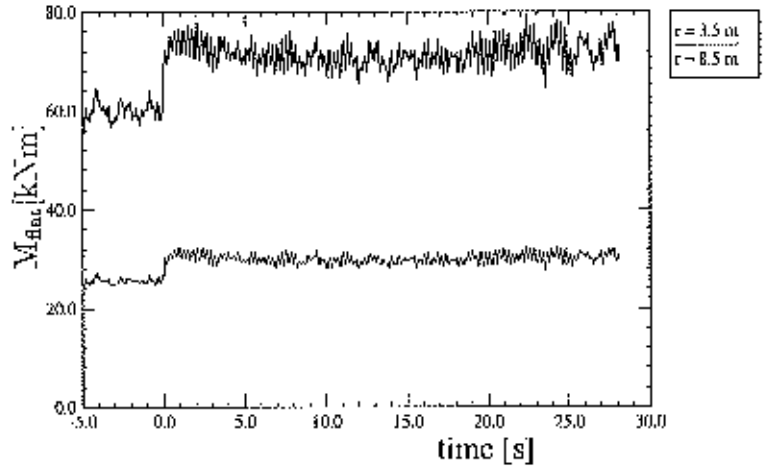

Figure 8.4 *WPS-30; Measured flat moment at blade root for step on the pitch angle going down, case WII_down*

the reason why in this report the case WI.2 and the WII results are discussed only.

Case WII is subdivided into the cases WII_up and case WII_down.

The description of the WPS-30 turbine is given in Appendix L.

8.2.1 Case WI.2

This case consisted of a very elementary calculation. The calculations were performed for stationary conditions and effects of wind shear, tilt angle and tower were not taken into account. Furthermore the effects of structural flexibility were neglected. The following conditions were assumed.

- V_∞ = 14.0 m/s;

- Pitch angle. A simple step on the pitch angle was prescribed:

$t(s)$	$\theta(^\circ)$
0.0	-1.5
5.0	-1.5
5.6	1.5
30.0	1.5
30.6	-1.5
60.0	-1.5

- Rotor speed is 44.0 rpm

Required as function of time:
- Axial induced velocities at r = 3.5 m (23% span), and r = 11.5 m (77 % span);
- Aerodynamic flatwise moments at r = 3.5 m (23% span) and r = 8.5 m (57 % span)
- Rotor shaft torque.

8.2.2 Case WII

The calculations were performed under constant wind conditions matching the average wind speed of the measured cases, and without wind shear, tilting angle or towershadow effects. The conditions for case WII_up are:
- V_∞ = 8.93 m/s ;
- Pitch angle: The measured pitch angle is prescribed, see figure 8.1. This pitch angle first remains constant at approximately -2.25 degrees, then it steps to -0.25 degrees. For readers who want to reproduce this case, the measured pitch angle time series is available on a floppy disc from the coordinator of the project upon request.
- Rotor speed = 36.1 rpm

The conditions for case WII_down are similar to those of case WII_up, but now the pitch angle is increased:
- V_∞ = 8.93 m/s ;
- Pitch angle: The measured pitch angle is prescribed, see figure 8.3. This pitch angle first remains constant at approximately -0.25 degrees, then it steps to -2.25 degrees. For readers who want to reproduce this case, the measured pitch angle time series is available on a floppy disc from the coordinator of the project upon request.
- Rotor speed = 36.1 rpm

For the cases WII, the following quantities were required as function of time:
- Axial induced velocities at r = 3.5 m (23% span), r = 8.5 m (57 % span), and r = 11.5 m (77% span);
- Flatwise moments at r = 3.5 m (23% span), and at r = 8.5 m (57% span); If possible effects of structural flexibility were taken into account.
- Rotor shaft torque.

8.3 Results of case WI.2 and WII

Discussion of results

The definition of these cases is given above, in section 8.2. The flatwise moments at two radial stations can be compared with measurements for case WII. Effects of structural flexibility are only taken into account by TUDk and ECN for case WII.

The results are presented in Appendix D.

Analysis of results

The calculated flatwise moment results show the well known overshoots from dynamic inflow effects, see the figures D.3, D.4, D.9, D.10, D.15 and D.16. In general the agreement between the calculations and the measurements for case W11 is good, but of course the comparison is obscured by the fluctuations in the measurements which are still present. Furthermore, it is reminded that the WPS-30 flatwise moment measurements have an unknown off-set, so attention should be paid to the dynamic ranges only.

When the results for the high wind speed case is compared with the result for the low wind speed case it can be seen that the overshoots for the high wind speed case are (relatively spoken) less. This was also found for the Tjæreborg turbine. The reason is that, although the rotor speed is higher at the high wind speed, the loading is lower by which the axial induction factors are also lower. For the 14 m/s case, the $\lambda = 4.93$ compared to $\lambda = 6.35$ for the 8.9 m/s case. In addition the loading at the low wind speed case is enhanced by the negative pitch angles. For the high wind speed case this leads to axial induction factors of 0.2 for the small pitch angle and 0.16 for the large pitch angle, compared to 0.32 resp. 0.25 at the low wind speed case.

It is clear that the overshoots are limited and they will in reality be dominated by load fluctuations from other sources (turbulence, wind shear, etc).

In the results of the induced velocities, it can be observed that generally spoken, the time scales of the ECN,de and the GH models are somewhat shorter than those in the free wake methods, see for example figure D.2. Furthermore the levels of the induced velocities calculated by the free wake methods are in general lower than those of the engineering methods, see for example figure D.8. This is in agreement with the results from [11].

It has been attempted to determine the time scale from the measured results in a similar way, as it was done from the data on the Tjæreborg turbine in the JOULE I project, see section 5.1.

The results (at a time 0.5 D/V_∞, after the start of the exponential recovery) are listed in table 8.2 for the flatwise moments at r = 3.5 m and at r = 8.5 m.

Table 8.2 *Time scale of the WPS-30 pitching step measurements*

case	r = 3.5m	r = 8.5m
W11_down	$0.65D/V_\infty$	$0.75D/V_\infty$
W11_up	$0.75D/V_\infty$	$0.45D/V_\infty$

It is emphasised that the determination of the time scale for the present measurements was even more difficult than it was for the Tjæreborg. This is due to the lower overshoots, by which, relatively spoken the load fluctuations due to turbulence and flexibility are larger. As explained in section 5.1, the determination of the time scale requires a smooth exponential function in which the values of F_1 and F_2 (see figure 5.3) are well defined.

The time scales of the flatwise moments at blade root, which are given in table 8.2 are between 0.65 and 0.75 D/V_∞. This is slightly higher than the values which were found in the JOULE I project, where the time scale was between 0.3 and 0.5 $D/V\infty$.

No consistant information can be obtained about the radial dependancy of the

time scale: For case WII_up the time scale at the most outboard station is smaller than at the inboard station but for case WII_down the time scale at the outboard position is larger. Probably the uncertainty in time scale determination is too large to draw a definite conclusion about the radial dependence of the time scale in the dynamic inflow process. It would be expected that at the tip, the time scale is shorter, due to the closer distance to the tip vortex.

Conclusions and recommendations

This section has shown that the dynamic inflow effects for the measurements which have been made on the WPS-30 turbine are smaller than for the Tjæreborg turbine. This is explained by the shorter time scale in the dynamic inflow process, due to the smaller turbine, while the pitching rate was approximately the same.

The overshoots in loads were, broadly speaking, predicted well with the dynamic inflow models. The time scale in the dynamic inflow process was found to be between approximately 0.65 and 0.75 D/V_∞.

9. AXIAL SYMMETRIC CASES, UNIWEX

9.1 Available measurements

In this section the pitching transients are described, which have been performed on the Uniwex turbine to further validate the models under axisymmetric conditions.

Both pitching step measurements and measurements of a stop procedure are supplied.

Measurements are available of the flapwise moment at r=1 m (12.5% span), and the flatwise moments at r=4m (50% span) and r=5.6m (70% span). The flatwise moments at the outboard sections are derived from strain gauges glued on the GRP blade material. The flapwise moment at r = 1.0 m is calculated from the strain measured in a load cell at a flapping cylinder.

In addition to the blade loads, the torque on the rotor shaft is measured. Furthermore, the pitch angle, the rotorspeed and the windconditions upstream of the turbine are available.

9.1.1 Measurement accuracy

The measurements on the Uniwex turbine which are described in this section have been carefully selected in order to have a good validation base for the project. It is believed that the recordings of the loads has been very accurate, both in terms of static and dynamic loads. Some off-set in the flatwise moments at the outboard stations (derived from the strain gauges on the blade) could be observed at final stand still of the stop campaign. This is probably caused by a temperature drift. The flapwise moment at the root (derived from the strains in the load cell of the flapping cylinder) hardly showed any drift.

All measurements which are reported in this section were made on one day and it is expected that the temperature drift during one day is very small. Therefore, the flatwise moments have all been corrected with the off-set from the stop measurement.

The measurements of the pitch angle, and the wind conditions are believed to be very accurate.

9.1.2 Discussion of pitching step measurements (case UI)

The figures 9.2 and 9.4 present the measured blade root flapwise moments for steps on the pitch angle from 2 to 8 degrees and from 12 to 18 degrees respectively. The figures 9.1 and 9.3 show the corresponding pitch angle time series. It must be noted that the time series which are presented in these figures are composed out of two different measurement series. The first measurement series consists of the step on the pitch angle going up. Then a separate measurement series for the step on the pitch angle going down, at conditions which may be slightly different, is appended. This leads to a small jump in loads at $t \approx 18$ s.

Every measurement series is averaged over 10 to 20 separate measurement series and over both blades in a similar way as it was done for the Tjæreborg turbine in the JOULE I project, see section 5.1. The pitching steps are from 2 to 8 degrees and from 12 to 18 degrees in about 0.4 seconds. The wind speed is about 8 m/s. The measurements at 50% blade span and 70% blade span are not discussed in this

section, but they are shown in Appendix B, together with the calculated results, see section 9.3.

Commonly, the Uniwex turbine is operated in variable speed mode, but for the present measurements, a constant rotor speed of about 49 rpm was applied. Similar to what was found at the WPS-30 turbine, see section 8.1.2, the rotor shaft torque was nevertheless clearly influenced by small fluctuations in the rotor speed, and therefore these measurements are not presented.

In table 9.1, the conditions of the measurements are summarized with the identification of the cases. The wind speed is the average value for the case, θ_1 is the initial and final blade pitch angle, θ_2 the intermediate one after the pitch step. The value of Δt gives the time in seconds used for both pitching changes. Also indicated in this table are calculated values of the equilibrium induction factors a_1 and a_2 at 70 % span, to give an indication of the loading situation. Although

Table 9.1 *Conditions of the Uniwex pitching step measurements*

case	λ [−]	V_∞ [m/s]	θ_1 [°]	θ_2 [°]	Δt [s]	a_1 [−]	a_2 [−]	Ω [rpm]
UI.1	5.73	7.97	8.0	2.0	0.4	0.094	0.11	49.2
UI.2	5.11	9.03	18.0	12.0	0.4	0.02	0.064	48.7

the measurements are taken at a medium wind speed, the loading is very small, due to the relatively low rotor speed. Furthermore the pitch angle refers to the twist from Appendix K, which is negative over a large part of the rotor blade: At the tip the twist angle is -5.1 degrees. This gives axial induction factors of 0.1 or even lower. This is considerable less than those for the WPS-30 measurements, see table 8.1 in section 8.1.2 and for the Tjæreborg measurements, see table 5.1 in section 5.1. In case UI.1, the flow is partly stalled over the rotor blade due to the relatively low pitch angle.

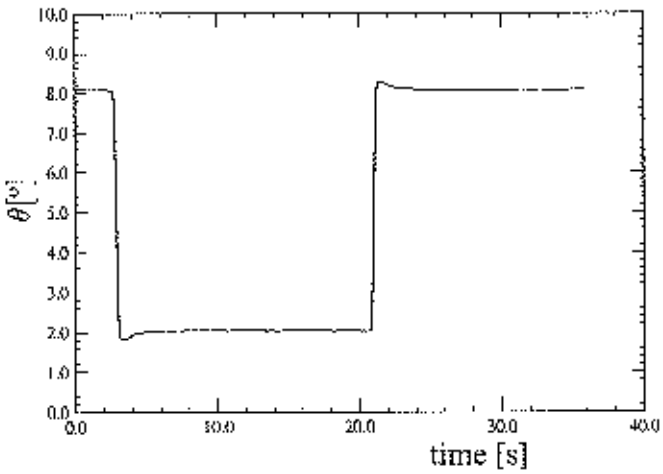

Figure 9.1 *Uniwex; Measured pitch angle for case UI.1 V_∞ = 7.97 m/s*

The figures 9.2 and 9.4 show only very small overshoots after the step on the pitch angle. This is partly due to the low loading, but it must also be noted that the time scale in the dynamic inflow process is an increasing function of rotor diameter (see also section 5.1). The pitching speeds in these experiments

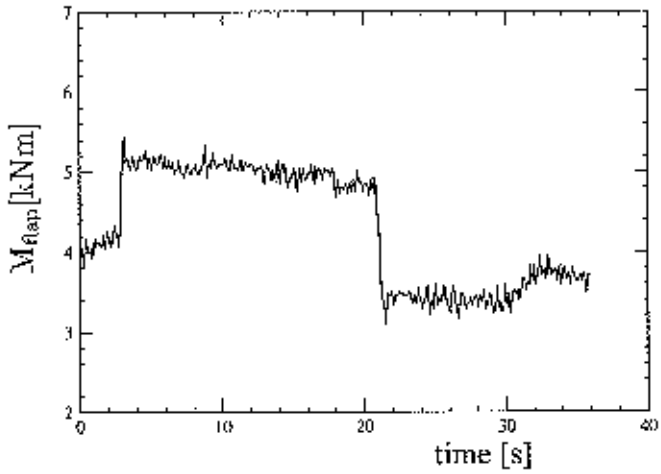

Figure 9.2 *Uniwex; Measured flap moment at blade root for step on the pitch angle, case UI.1*

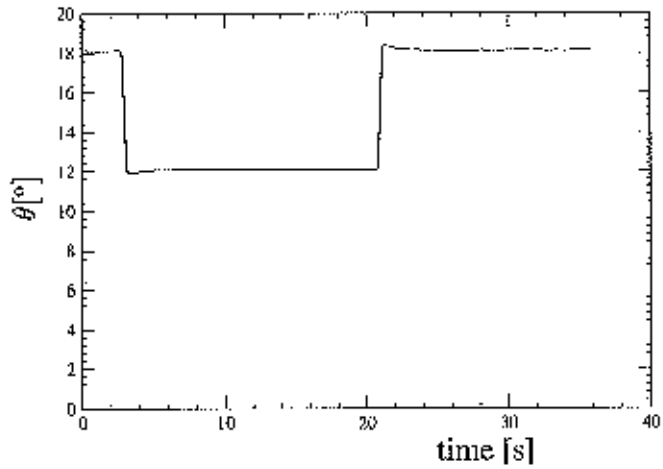

Figure 9.3 *Uniwex; Measured pitch angle for case UI.2;* V_∞ *= 9.03 m/s*

were not proportionally scaled compared to the Tjaereborg measurements and as a consequence the overshoots in the loads appear smaller for this smaller scale machines.

A comparison with the WPS-30 turbine pitching steps is difficult to make due to the large fluctuations which are present in the time series. The overshoots in the flatwise moment at blade root, for the step down on the WPS-30 turbine, see figure 8.4 is (related to the mean load level) estimated to be 4/75 ≈ 5.3%. For the flapwise moment at blade root of the step down on the Uniwex turbine, see figures 9.2 and 9.4, the overshoots are estimated to be 0.4/6 = 6.67% and 0.4/4 = 10%. Although these overshoots are larger than for the WPS-30 turbine, it must be borne in mind that also the pitching speed and the pitching step are considerable larger for the Uniwex turbine.

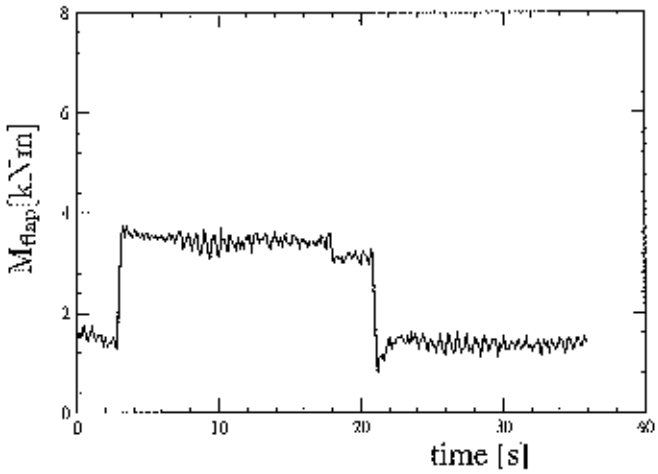

Figure 9.4 *Uniwex; Measured flap moment at blade root for step on the pitch angle, case UI.2*

9.1.3 Discussion of stop measurements (case UIII)

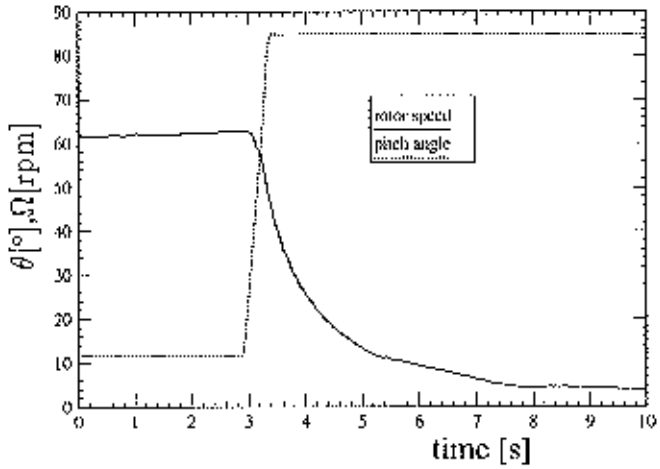

Figure 9.5 *Uniwex; Measured pitch angle and rotor speed for stop, case UIII,* $V_\infty \approx$ *11.867 m/s*

Figure 9.6 shows the measured blade root flapwise moments during a stop of the Uniwex turbine.

The measured flapwise moments have been averaged over the number of blades, in order to filter out the effects of wind shear.

In figure 9.5 it is seen that the blade is feathered from 11.6 to 84.5 degrees pitch angle at a fast (approximately constant) pitching rate of about 150 degrees/seconds. In this figure, the rotor speed is presented also. As soon as the drive train has become free, the rotor begins to decelerate, and the drive train exhibits a strong vibration.

A further discussion of this case, takes place in section 9.3.2, where the measured data are compared with calculational results.

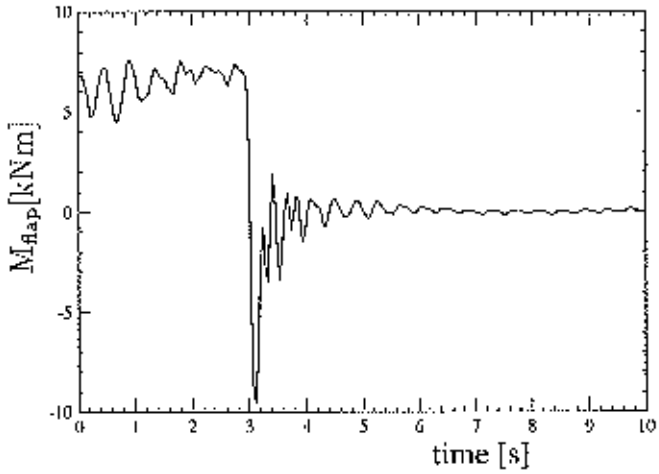

Figure 9.6 *Uniwex: Measured blade root flapwise moment for stop, case UIII,* $V_\infty \approx$ *11.867 m/s*

9.2 Definition of calculation cases

9.2.1 Pitching steps (Case UI)

The pitching step cases on the Uniwex turbine are denoted by case UI.1 and UI.2.

The description of the Uniwex turbine is given in Appendix K.

The calculations were performed under constant wind conditions matching the average wind speed of the measured cases, and without wind shear, tilting angle or tower shadow effects. The conditions for case UI.1 are:

- V_∞ = 7.97 m/s ;
- Pitch angle: The measured pitch angle is prescribed, see figure 9.1. This pitch angle first remains constant at approximately 8 degrees, then it steps to 2 degrees after which it returns to 8 degrees.
- Some participants used the measured rotor speed, others a constant rotor speed of 49.19 rpm.

The conditions for case UI.2 are:

- V_∞ = 9.03 m/s ;
- Pitch angle: The measured pitch angle is prescribed, see figure 9.3. This pitch angle first remains constant at approximately 18 degrees, then it steps to 12 degrees after which it returns to 18 degrees.
- Some participants used the measured rotor speed, others a constant rotor speed of 48.68 rpm

For readers who want to reproduce this case, the measured pitch angle and rotor speed time series are available on a floppy disc from the coordinator of the project upon request.

For both cases, the following quantities were required as function of time:

- Axial induced velocities at r = 2 m (25% span), r = 4 m, (50% span) and r = 5.6 m (70% span);
- Flapwise (out of rotor plane) moments at r = 1 m (12.5% span), and flatwise (out of chord) moments at r = 4 m (50% span) and r = 5.6 m (70% span); If possible effects of structural flexibility were taken into account.
- Rotor shaft torque.

9.2.2 Stop case (Case UIII)

The stop case on the Uniwex turbine is denoted by case UIII

Since the measured flatwise moments are averaged over the number of blades, the calculations were performed under constant wind conditions matching the average wind speed of the measured cases, and without wind shear, tilting angle or tower shadow effects,

The description of the Uniwex turbine is given in Appendix K.

The conditions for case UIII are:
- V_∞ = 11.867 m/s;
- Pitch angle: The measured pitch angle is prescribed, see figure 9.5.
- Rotor speed: The measured rotor speed was prescribed, see figure 9.5.

For readers who want to reproduce this case, the measured pitch angle and rotor speed time series are available on a floppy disc from the coordinator of the project upon request.

The following quantities were required as function of time:
- Axial induced velocities at r = 2 m (25% span), r = 4 m, (50% span) and r = 5.6 m (70% span);
- Flapwise (out of rotor plane) moments at r = 1 m (12.5% span), and flatwise (out of chord) moments at r = 4 m (50% span) and r = 5.6 m (70% span); If possible effects of structural flexibility were taken into account.
- Rotor shaft torque.

9.3 Results

9.3.1 Results of pitching steps (case UI)

Discussion of results

The definition of this case is given above, in section 9.2. The flatwise (or flapwise) moments at three radial stations can be compared with measurements. Effects of structural flexibility are only taken into account by TUDk.

The results are presented in Appendix B. DUT only supplied case UI.2, because case UI.1 was obscured by the stalled conditions on the blade, the modelling of which was outside the scope of the project.

Analysis of results

In the figures B.1, B.2, B.3, B.8, B.9 and B.3 the results of the induced velocities are presented. All calculated induced velocities are on a low level and undergo only very small changes due to the step on the pitch angle. It must be noted that for case UI.1 the rotor blade is partly stalled, by which the agreement between calculations and measurements is mainly determined by uncertainty in stall modelling. This kind of modelling is outside the scope of the present project.

Nevertheless, some differences are apparent, which can be related to the dynamic inflow modelling. When comparing the induced velocity results from the engineering methods with the results from the more advanced Unist. and NTUA free wake methods it can be observed that the time constant from the ECN,de model and the GH model is somewhat shorter, see for example figure B.9. This was also found for the WPS-30 results, see section 8.3.

The fluctuations in the induced velocities from DUT, Unist and NTUA, can be explained by the influence of the tip vortex which is shed from the previous blade.

The induced velocities predicted by the free wake methods from Unist. and NTUA, for the non-stalled case UI.2 are in general on a lower level than those from the engineering methods, in agreement with the results from [1].

The consequences of the discrepancies in the induced velocities on the loads are small. In general a good agreement between the calculations and the measurements, and between the calculations mutually is found. The overshoots in measured loads which are discussed in section 9.1.2 are also present in the calculated results but it must be noted that in practice, these overshoots are fully dominated, by load fluctuations from other sources (turbulence, wind shear, etc).

Some differences can be observed in the mean level of the loads: The lower values from TUDk can be explained by the centrifugal stiffening effect, since TUDk is the only party which accounts for structural dynamics. Furthermore the flatwise moments of DUT are generally on a lower level.

It is also remarkable to see that in figure B.7, most participants predict a decrease in rotor shaft torque from the increase in pitch angle, where the flatwise moments show an increase. This is probably caused by the increase in profile drag in the stall region. The profile drag influences the flatwise moments to a much smaller degree. The NTUA model cannot deal stall, which is why they show an increase in rotor shaft torque with increase in pitch angle.

As for the Tjæreborg and the WPS-30 turbine (see the sections 5.1 and 8.3), the time scale, has again been determined from the measured flapwise moments at a time Δ t = 0.5 D/U after the start of the exponential recovery. The determination of the time scale for the present measurements Uniwex was again extremely difficult. This is due to the very low overshoots, by which, relatively spoken the load fluctuations due to turbulence and flexibility are larger. Nevertheless the procedure which has been described in [1] is applied to get a rough estimate for the time scale. The results of the time scale at a time of 0.5 D/V after the start of the exponential recovery are listed in table 9.2. The results are given for both cases, at all three radial stations, and for the step of the pitch angle going up and the step going down. For case UI.2, the overshoot in flatwise moment at the 4 m station was too small to get a realistic time scale.

Table 9.2 *Time scale of the Uniwex pitching step measurements*

case	r = 1m	r = 4m	r = 5.6m
UI.1 step down	$0.35D/V_\infty$	$0.5D/V_\infty$	$0.5D/V_\infty$
UI.1 step up	$0.2D/V_\infty$	$0.2D/V_\infty$	$0.25D/V_\infty$
UI.2 step down	$0.5D/V_\infty$	n.r.	$0.6D/V_\infty$
UI.2 step up	$0.3D/V_\infty$	$0.4D/V_\infty$	$0.25D/V_\infty$

The time scales of the flapwise moments at blade root are between 0.2 and 0.5 D/V_∞. This compares reasonable well with the values which were found in the JOULE I project, where the time scale was between 0.3 and 0.5 D/V_∞. As explained in section 8.3, it would be expected that towards the tip, the time scale decreases: Due to the closer distance to the tip vortex, the time which is needed to be influenced by a sudden change in tip vorticity is shorter. However, in some cases, the time scale at the tip is larger. This may be due to the uncertainty in time

scale determination, which is too large to find the dependency of the time scale on the radial distance.

Conclusions and recommendations
This section has shown that the dynamic inflow effects are very small in the measurements which have been made on the Uniwex turbine. This is explained by the low loading at the measurement cases, but also by the shorter time scale due to the small size of the turbine. Nevertheless, some overshoots in loads are observed, which can be attributed to dynamic inflow. The agreement between the calculated and measured blade loads was broadly speaking, well. The time scale in the dynamic inflow process was found to be between approximately 0.2 and 0.5 D/V_∞.

9.3.2 Results of stop case (case UIII)

Discussion of results
The definition of this case is given above, in section 9.2. The flatwise (or flapwise) moments at three radial stations can be compared with measurements. In addition, the calculation of the rotor shaft torque is compared with measurements.

Effects of structural flexibility are taken into account by ECN, TUDk and GH. GH did not calculate the flatwise moments at the outboard stations for the stop case. As described in Appendix K, TUDk adjusted the mass and stiffness distributions, to obtain the correct eigenfrequencies from a simple beam- model.

The results are presented in Appendix C. The period from t = 2s to t = 5s is presented only. This is the most interesting period during which the stop takes place.

Analysis of results
In the figures C.1 to C.3, the results of the induced velocities are presented. In the period prior to the pitch feathering, the induced velocities are on a constant level. When the stop is initiated and the blade starts to pitch, the induced velocity decreases and becomes (slightly) negative in most cases.

In most results, the decrease in induced velocity is in phase with the decrease in pitch angle (from t = 2.9 s to t = 3.4 s). The only difference is in the TA result, which gives a much slower decrease in induced velocity. This indicates that the dynamic inflow effects on the loads are very limited: If these effects were very pronounced the induced velocities would lag behind the pitch angle. The explanation is the short time scale for the Uniwex turbine. In the previous section a time scale of about 0.6 s is found for this wind speed. In addition it was shown in [1], that even at a stop of a large turbine, the dynamic inflow effects in terms of load overshoots are often small. The maximum(minimum) loads during a stop are in most cases determined by the minimum stall value of the litt coefficient. Usually, the only difference due to dynamic inflow is the time at which negative stall is reached. However the time at which negative stall is reached does not have much impact on the load overshoot and consequently a calculation with and without dynamic inflow yields the same maximum(minimum) load, but at a different time. In cases with low pitching rates, dynamic inflow may be of more importance. In such situations, the minimum lift coefficient may not be reached in an equilibrium wake calculation, but through dynamic inflow effects it is reached.

The calculational results of the flatwise moments from the DUT model give less overshoots, see the figures C.4 to C.6. The explanation is the structural dynamic effects, which is taken into account by the other participants which are presented in these figures. A calculation with the ECN,de model without flexibility yields the same overshoot.
The fluctuations which are visible in the measured flatwise moments are reproduced quite well with the models which have included structural dynamic effects.

The differences which are apparent in the rotor shaft torque results in figure C.7 are explained by the fact that some participants calculate the aerodynamic torque (which becomes negative and decelerates the rotor) where other participants have calculated the total torque, which is approximately zero when the drive train is running freely.

Conclusions and recommendations
This section has shown that for the Uniwex stop case, the dynamic inflow effects on the loads are very small. The explanation is the short time scale for this small turbine. In addition, the extreme loads during a stop are mainly determined by the minimum lift coefficient. In most cases the minimum lift coefficient is reached whether dynamic inflow effects are account for, or not.

10. PITCHING STEP CASES, WINDTUNNEL

10.1 Available measurements

In this section the pitching step measurements are described, which have been recorded in the DUT wind tunnel.

Despite the well known disadvantage, inherent to wind tunnel measurements, which are due to scaling effects between the small wind turbine model and a full size wind turbine, the measurements in the windtunnel have two important advantages:

1. The wind tunnel offers a more controlled environment. Although the turbulence level in the tunnel environment is 0.8%, and consequently not completely negligible, the load fluctuations due to turbulence, are very small. It is reminded that the extraction of the relevant dynamic inflow fluctuations in full scale was difficult, due to the unknown turbulent fluctuations
2. In the wind tunnel, the flow field in the wake was recorded during the pitching steps. For all full scale experiments, the blade and rotor loads were measured only, which delivered indirect validation material for the dynamic inflow models. The flow field measurements in the wind tunnel give more direct information about the dynamic inflow processes in the wake which influence the loading in the rotor plane.

10.1.1 Generation of pitch angle steps

The change in blade pitch angle is established by incorporating fast motors in the hub, which control the pitch axis of the blade. The motors are actuated by means of a PC-based controller system.

With the use of these fast motors, a change in blade pitch angle of 400°/s is reached.

10.1.2 Measurement accuracy

Some comments on the measurement accuracy are given in [1]. It is believed that the present measurements of static and dynamic loads, pitch angle and wind speed are very accurate. However it must be noted, that although the measurements are taken in a wind tunnel environment, the non-uniformity and turbulence may still be notable in the measurements.

10.1.3 Discussion of measured pitching steps (cases tun-pitch)

Three measurement series at different tunnel conditions are available. The time series of the pitch angles are presented in the figures 10.1, 10.5, and 10.9. It can be seen that the pitching steps for all these measurement series are almost similar.

The pitching steps are from +2 to -2 degrees at tunnel speeds of 5.03 m/s ($\lambda = 7.5$), 3.77 m/s ($\lambda = 10.0$) and 7.54 m/s ($\lambda = 5$). In these pitching steps, after an initial period of 0.5 seconds, the blade pitch angle is decreased with a very fast rate of about 400°/s, then it remains constant over a period of 1 second after which it returns to its initial value, again with a very fast pitch rate. Note that there is a small overshoot in the pitch angle after every step. The very fast pitching speed implies that the pitching steps could be performed within approximately